THESIS FOR THE DEGREE OF DOCTOR OF PHILOSOPHY

Drip Sealing Grouting of Tunnels in Crystalline Rock: Conceptualisation and Technical Strategies

CHRISTIAN BUTRON

Department of Civil and Environmental Engineering
Division of GeoEngineering
CHALMERS UNIVERSITY OF TECHNOLOGY
Gothenburg, Sweden 2012

Drip Sealing of Tunnels in Crystalline Rock: Conceptualisation and Technical Strategies
CHRISTIAN BUTRON
Department of Civil and Environmental Engineering
Division of GeoEngineering
Chalmers University of Technology

ABSTRACT

A conceptual model of the groundwater hydraulic conditions around the tunnel contour in ancient brittle crystalline rocks has been developed and verified. The general aim has been to reach an understanding of the groundwater conditions in and close to the tunnel roof where dripping takes place and to propose technical and practical strategies for waterproofing. Dripping is accompanied by ice growth and icicle formation in cold regions, creating additional problems such as shotcrete fall-outs, icicle fall-outs, damage to vehicles, damage to trains, etc.

The methodology for the development of the conceptual model is based mainly on transmissivity determinations from short-duration hydraulic tests and analyses of the connectivity of the fracture structure by means of semi-variogram analysis. The determination of the dimensionality of the flow in the fractures has also been found to be essential in order to describe the conductive system. This conceptual model describes the fracture systems as a combination of transmissive patches (2D-flow fractures) connected by less pervious channels (1D-flow fractures). It provides an understanding of the heterogeneity and connectivity of the fracture network and thus the groundwater conditions, not only in the roof but also around the tunnel contour.

The pre-excavation grouting design process used in the tunnelling projects followed a structured approach and the evaluation showed that the grouting design reduced the inflow and fulfilled the environmental demands. However, dripping remained, making its characterisation very important when proposing a possible solution for its control. It is proposed that the remaining dripping comes from a channelised system that has been left unsealed and which would be extremely difficult to intersect with future boreholes, as well as from some ungrouted fractures with inconvenient orientations. Geomembrane lining and post-excavation grouting are possible solutions, although particular attention needs to be given to the location. With the proper grouting technique and knowledge of the fracture system and hydrogeology, it is possible to propose technical strategies for waterproofing a tunnel roof.

Keywords: Grouting, design, evaluation, crystalline rock, drip sealing, unsaturated flow, ice growth, icicle formation, rock fracture, channels, dripping.

Christian Butrón

LIST OF PUBLICATIONS

This thesis includes and is based on the work contained in the following publications, referred to by Roman numerals:

I.   **Butrón C.**, Axelsson M. and Gustafson G. (2009). Silica sol for rock grouting: Laboratory testing of strength, fracture behaviour and hydraulic conductivity. Tunnelling and Underground Space Technology, Vol. 24, No. 6, pp. 603-607.

II: **Butrón C.**, Gustafson G., Fransson Å. and Funehag F. (2010). Drip sealing of tunnels in hard rock: A new concept for the design and evaluation of permeation grouting. Tunnelling and Underground Space Technology, Vol. 25, No. 2, pp. 114-121.

III: Gustafson G., **Butrón C.** and Fransson Å., (2008). Characterisation of the hydraulic properties of fractured rock from grouting data. Proceedings of the 36th IAH Congress – Integrating Groundwater Science and Human Well-Being, Toyama, Japan, pp. 1721-1728.

IV: **Butron C.** (2009). Drip sealing of tunnels in crystalline rock: Pre-excavation design and evaluation. Licentiate Thesis, Chalmers University of Technology, Gothenburg, Sweden.

V: **Butrón C.**, Gustafson G. and Funehag J. (2009). Assessment of the transmissivity field in fractured rock: A case study in the TASS Tunnel. Nordic Symposium of Rock Grouting, Helsinki, Finland, pp. 109-117.

VI: Hernqvist L., **Butrón C.**, Fransson Å., Gustafson G. and Funehag F. (2011). A hard rock tunnel case study: Characterisation of the water-bearing fracture system for tunnel grouting. Accepted for publication in Tunnelling and Underground Space Technology.

VII: **Butrón C.**, Funehag F. and Gustafson G. (2010). How impermeable can a tunnel get? A case study with drip mapping as a method. Proceedings of the 11th IAEG Congress – Geologically Active, Auckland, New Zealand, pp. 2711-2719.

A report on the pre-excavation grouting design and evaluation of the Sjökullen Tunnels was being revised at the time this thesis was presented. Due to the recent completion of the project, it is not included as a publication although the data collected and observations from the project are used in this thesis.

Division of work between authors

In Publication I, Butrón, Axelsson and Gustafson defined the aim and scope. The starting point of the work was a report written by Axelsson (Axelsson, 2004) and a master's thesis written by Butrón (Butrón, 2005). Butrón performed the laboratory tests and was the main author of the publication with support from the other authors.

In Publication II, Butrón and Gustafson developed the grouting design concept and Butrón, with the support of Funehag, monitored the grouting procedure in the field. Butrón was the main author of the publication with support from the other authors.

In Publication III, the aim and scope were defined by Gustafson, Butrón and Fransson. Butrón performed the variogram and kriging analyses. Gustafson was the main author of the publication, with support from the other authors. The publication was presented as a poster at the 36th IAH Congress in Toyama, Japan and in addition to being published in the conference proceedings book it also received an award.

Publication IV is the author's licentiate thesis. It was a summary of the PhD project, written thus far by Butrón with support from the supervisors Gustafson and Fransson. Only the abstract is included in this doctoral thesis.

In Publication V, the aim and scope were defined by Butrón in collaboration with Gustafson. Butrón performed the variogram and kriging analyses and was the main author of the publication. Funehag supplied the data from the tunnel grouting project. The publication was presented by Butrón at the Nordic Symposium of Rock Grouting in Helsinki, Finland, and is included in the conference proceedings book.

In Publication VI, the aim and scope were defined by Hernqvist, Butrón, Gustafson and Fransson. Hernqvist performed the hydraulic evaluations. Butrón performed the variogram and kriging analyses. Funehag supplied the data from the tunnel grouting project. Hernqvist was the main author, with support from the other authors.

In Publication VII, the aim and scope were defined by Butrón in collaboration with Funehag. Butrón conducted the fieldwork and was the main author of the publication with support from the other authors. The publication was included in the conference proceedings book at the 11th IAEG Congress in Auckland, New Zealand.

Christian Butrón

ACKNOWLEDGMENTS

Christian Butrón

x

TABLE OF CONTENTS

LIST OF NOTATIONS

The following notations are used in the main text of the thesis:

Roman letters

A	[m^2]	Area
B	[m]	Section length
b	[m]	Hydraulic aperture
b_{crit}	[m]	Critical hydraulic aperture for grout penetration
b_r	[m]	Given hydraulic aperture
C	[m^2·m/s]	Conductance
d	[m]	Diameter of a circular cross-section channel
d_{95}	[m]	Grain diameter of grout that 95% of the grain distribution is smaller than
g	[m/s^2]	Earth's acceleration, 9.81 m/s^2
H	[m]	Water table distance to tunnel
h	[m]	Lag distance
K	[m/s]	Hydraulic conductivity
k	[-]	Pareto distribution coefficient
l, L	[m]	Length
n	[-]	Size order number
p_w	[N/m^2]	Groundwater pressure
P_c	[Pa]	Capillary pressure
Q	[m^3/s]	Inflow
Q_{mom}	[m^3/s]	Momentaneous flow
$q_{grouted}$	[m^3/s/m]	Water inflow per unit width into an ideally grouted tunnel
r	[-]	Rank
S	[-]	Saturation
T	[m^2/s]	Transmissivity
T_r	[m^2/s]	Given transmissivity
t	[s]	Time
t_G	[s]	Gel induction time
V	[m^3]	Volume
w	[m]	width

z	[m]	Elevation above a vertical datum

Greek letters

μ	[Pa·s]	Fluid dynamic viscosity
ρ	[kg/m^3]	Fluid density
τ_o	[Pa]	Fluid initial yield stress
ψ	[Pa]	Pressure head
Θ	[m^3]	Water content

Mathematical expressions

dh	[m]	Difference in hydraulic head
dh/dx, dh/dl	[m/m]	Hydraulic gradient
Q/dh	[m^2/s]	Specific capacity
$\gamma(h)$	[-]	Variogram function
$N(h)$	[-]	Observation pairs
$Z(x)$	[-]	Observation value
Δp	[N/m^2]	Applied overpressure

Acronyms

AFTES	Association Française des Travaux en Souterrain
EDZ	Excavation damaged zone
ITA	International Tunnelling Association
NIT	Natural inflow test
PVT	Pressure, volume, time
WPT	Water pressure test
Äspö HRL	Äspö Hard Rock Laboratory

1   INTRODUCTION

This chapter addresses and summarizes the problem and states the aim and objectives of this thesis. The scope of work that presents the main steps followed in this investigation is illustrated and explained, and the limitations of the thesis are addressed.

1.1   Background

In tunnels constructed below the groundwater level, water inflow is a problem during and after construction. According to, among others, Richards (1998) and Asakura and Kojima (2003), it is the main reason for repair, maintenance and upgrading work. The scale of these problems depends on the site condition, construction method and amount of inflow. According to the ITA Working Group on Maintenance and Repair of Underground Structures (1991), high inflows are expected to cause damage inside and surrounding the tunnel, resulting in low inflows into the facility and affecting the functionality of the tunnel.

Normally in Scandinavia, pre-excavation grouting is used as a method to control high inflows into the tunnel, satisfying in most cases the environmental demands set in the different projects. However, low inflows, such as dripping, are not yet controlled by pre-excavation grouting. An improvement to the sealing effect obtained by the pre-excavation grouting can be obtained by post-excavation grouting although it is common that dripping remains, leaving the installation of geomembranes as an additional measure. Both post-excavation grouting and the use of geomembranes are expensive remedial measures and increase the construction cost and the maintenance work, which a tunnel owner would like to avoid.

According to Richards (1998), Asakura and Kojima (2003), the AFTES Working Group No. 14 (1989) and the ITA Working Group on Maintenance and Repair of Underground Structures (1991), dripping is accompanied by ice growth and icicle formation in cold regions, creating additional problems such as shotcrete fallouts, rock fallouts, icicle fallouts, tunnel deformation, reduction of the tunnel opening due to ice barriers, icing of the road surface in road tunnels, obstruction of ventilation by ice, damage to vehicles, damage to trains, damage to the lining and damage to the appearance. According to Andrén (2006) and Andrén (2008)

many tunnels in Sweden reveal these problems and require extensive maintenance. Dripping control is therefore imperative in tunnel construction.

All these problems highlight the importance of well-conducted pre-excavation grouting as an early counter-measure, not only to reduce water leakage to specific levels but also to reduce dripping, ice growth and icicle formation. A drip sealing grouting design will thus help to reduce the dripping and the number of counter-measures during and after the construction of tunnels. In some cases, pre-excavation grouting should be complemented with post-excavation grouting, depending on the site conditions, to guarantee that the tunnel is as watertight as possible.

1.2   Aim and objectives

Based on the background, it is clear that dripping is a persistent problem and that in cold regions the problems are made worse by the growth of ice and formation of icicles. Not only does this affect the construction stage, it also increases maintenance work during the lifetime of the tunnel. The overall aim of this thesis is to reach an understanding of the groundwater conditions in and close to the tunnel roof where dripping takes place and to propose technical and practical strategies for waterproofing the tunnel roof.

The thesis has the following specific objectives in addition to the overall aim:

- To develop and verify a conceptual model of the conductive fracture system before and after excavation for drip sealing grouting purposes.
- To the present different drip sealing grouting design approaches conducted and their evaluations.
- Suggest further measures to stop the remaining dripping after grouting based on its characterisation and the subsequently developed conceptual model.

1.3   Scope of work

The scope of work can be described in the following steps, presented in Figure 1.1. Firstly, a literature review was carried out. The review is presented in a published Licentiate Thesis (Publication IV). Laboratory tests were then conducted on the properties of silica sol as a suitable grout for drip sealing and the results are presented in Publication I.

Assuming that fractures behave similarly to smooth parallel plates, a first drip sealing grouting design approach for a tunnel, the Nygård Tunnel, was conducted and is presented in Publication II. Based on the results obtained from the grouting procedure in the Nygård Tunnel, a conceptual model of the conductive fracture system before grouting was addressed and this is presented in Publication III.

The further application of a drip sealing grouting design in two additional tunnels, the TASS Tunnel and the Sjökullen Tunnels, is presented in Chapter 5. The conceptual model was then verified by the results obtained from the grouting procedure conducted in the TASS Tunnel, which is presented in Publications V and VI. An analysis of the remaining dripping was made and is presented in Publication VII and Chapter 6. This analysis helps to understand the flow conditions in the tunnel contour after grouting and with the aid of some laboratory observations obtain a comprehensive picture of the flow conditions in and close to the tunnel roof.

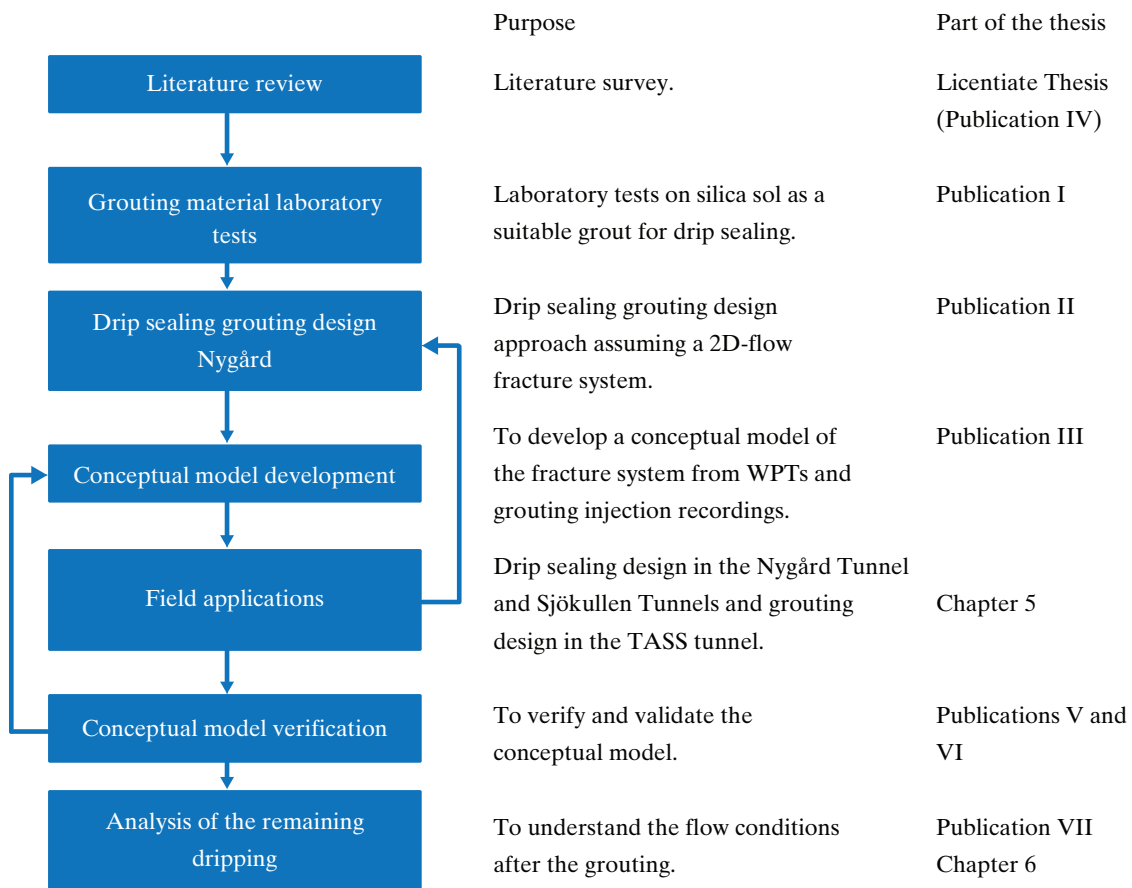|	Purpose	Part of the thesis
Literature review	Literature survey.	Licentiate Thesis (Publication IV)
Grouting material laboratory tests	Laboratory tests on silica sol as a suitable grout for drip sealing.	Publication I
Drip sealing grouting design Nygård	Drip sealing grouting design approach assuming a 2D-flow fracture system.	Publication II
Conceptual model development	To develop a conceptual model of the fracture system from WPTs and grouting injection recordings.	Publication III
Field applications	Drip sealing design in the Nygård Tunnel and Sjökullen Tunnels and grouting design in the TASS tunnel.	Chapter 5
Conceptual model verification	To verify and validate the conceptual model.	Publications V and VI
Analysis of the remaining dripping	To understand the flow conditions after the grouting.	Publication VII Chapter 6

Figure 1.1   Schematic description of the scope of work and the publications that deal with the specific parts of this thesis.

Drip sealing grouting field tests were conducted on two railway tunnels, the Nygård Tunnel and the Sjökullen Tunnels, located in the western part of Sweden and part of the "BanaVäg i Väst" project, which is being expanded to improve accessibility, see Figure 1.2. The Nygård Tunnel is located 40 to 50 m below ground and is approximately 3 km long, of 86 m were tested. The Sjökullen Tunnels are located between 10 and 15 m below the ground surface and are 120 m long.
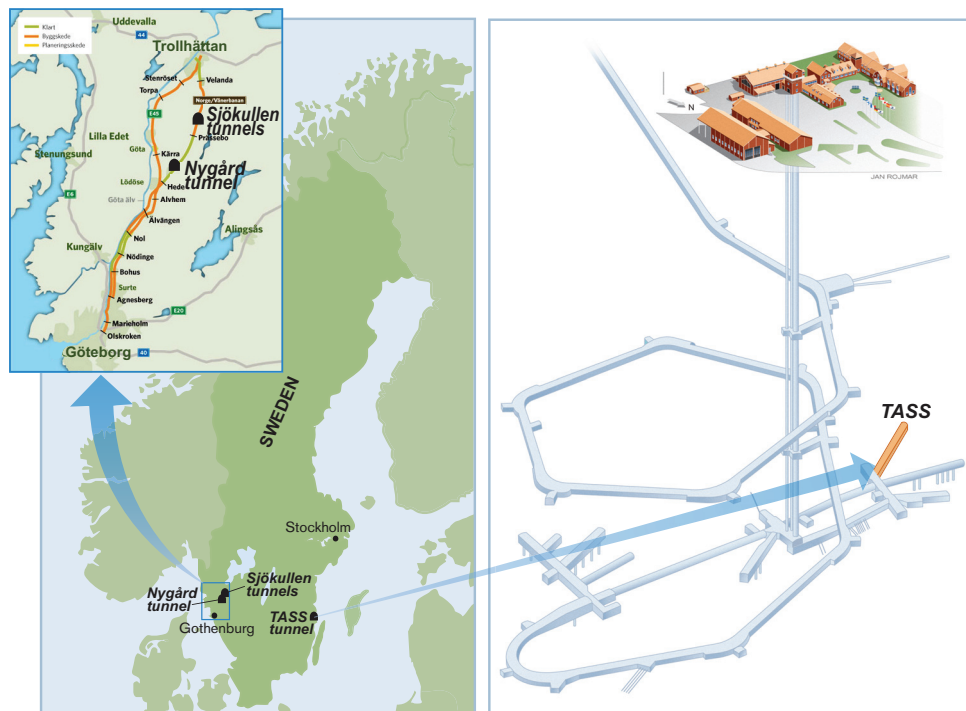
Figure 1.2   *Location of the two case study tunnel projects: To the left, the location of the Nygård Tunnel and the Sjökullen Tunnels (Trafikverket, 2011a). To the right, the location of the TASS Tunnel at Äspö Hard Rock Laboratory (Äspö HRL). Source: SKB, illustrator: Jan Rojmar, slightly modified.*

A third field test was also conducted at the TASS Tunnel at the Äspö Hard Rock Laboratory (Äspö HRL). Äspö HRL is situated north of Oskarshamn, on the east coast of Sweden. The tunnel is 450 m below ground and is associated with research for spent nuclear fuel repositories, see Figure 1.2. In this field test, the remaining dripping was mapped and measured following excavation of the tunnel "dripping characterisation". The complete grouting procedure in the TASS Tunnel can be explored in detail in Funehag (2008) and Funehag and Emmelin (2011).

1.4 Limitations

When dealing with permeation grouting of underground constructions, it is impossible to include all aspects of host rocks. This thesis therefore focuses on tunnels constructed in crystalline rock, below the groundwater table and assuming negligible matrix flow. However, the conceptualisation, characterisation and design could be applied to tunnels constructed in other types of fractured rock. Rock mechanical aspects are not covered by this thesis and grouting is used as a means of waterproofing and not stabilisation. During the grouting design phase of the Nygård Tunnel and the Sjökullen Tunnels due account was taken of limitations in the form of equipment, time, financial matters and contractual issues although these are not addressed in this thesis

2   THEORETICAL BACKGROUND

This chapter provides a brief theoretical foundation to help the reader understand the rest of the thesis. Particular attention is given to the bases needed to construct the conceptual models presented in the next chapter. Some of this text has been taken directly or reformulated from the Licentiate thesis, which comprises a literature review. A basic description of the grouting design parameters and technique, and the conditions for water flow at temperatures below zero are covered in the Licentiate thesis and some practical implications are commented on briefly in the discussion section.

2.1   Description of a rock fracture

Crystalline rocks, whether of igneous or metamorphic origin, have low porosity, and groundwater flows mainly through the open fractures, see e.g., Fetter (2001), and is thus a common reason to assume negligible matrix flow. Fractures vary in length, aperture and void geometry, and the reason for or extent of these variations are influenced by the origin, age and stress history of the rock being studied, see e.g., Warner (2004). Chernyshev and Dearman (1991) define a fracture as a complex-shaped cavity filled with gas, liquid and/or solid mineral matter and differentiate it from pores and solution cavities in that their length far exceeds their width or aperture, see Figure 2.1. An example of a basic conceptual interpretation of a real longitudinal fracture section is shown in Figure 2.1 (Winberg et al., 2000).

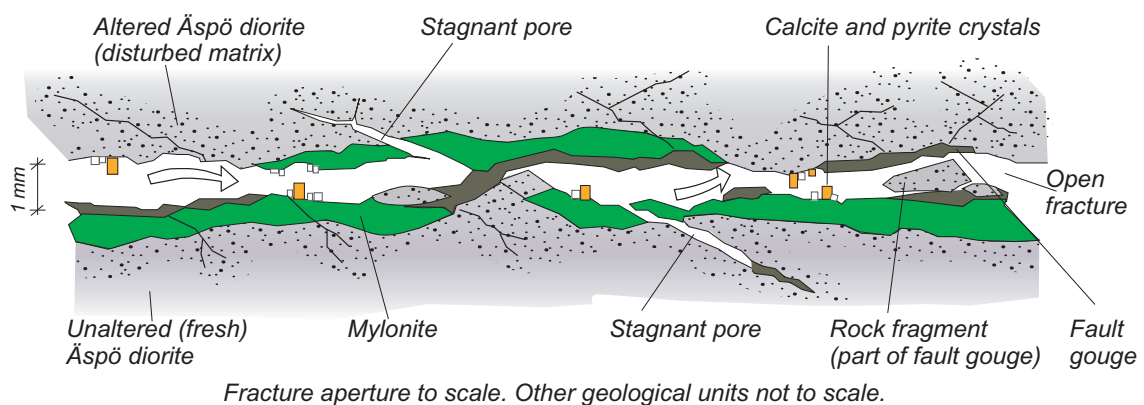*Fracture aperture to scale. Other geological units not to scale.*

Figure 2.1   *Basic conceptual interpretation of a longitudinal fracture section at Äspö HRL. The model shows a fracture where the length is larger than the varying aperture. The fracture aperture is to scale but other geological units are not. Modified from Winberg et al. (2000).*

2.2 Flow in a fracture

The relationship between the flow, Q, and the hydraulic aperture, b, assuming that the previous described fracture resembles two smooth parallel planes with a width, w, is obtained using the cubic law, Equation 2.1, (Snow, 1969, see de Marsily, 1986).

$$Q = -\frac{dh}{dl} \cdot \frac{\rho \cdot g}{\mu} \cdot \frac{w \cdot b^3}{12} \tag{2.1}$$

Distinctively, the hydraulic aperture of a fracture could vary from microns to a few millimetres, significantly affecting the transmissivity of the rock mass as the transmissivity in a single fracture increases as the cube of its opening. The parameters used are the fluid density, ρ, earth acceleration, g, hydraulic gradient, dh/dl, and the fluid dynamic viscosity, μ.

2.3 Flow through a circular tube

When extreme channelling is considered instead, the relationship between the flow, Q, through a cylindrical tube with constant circular cross-section and its diameter, d, and hydraulic gradient, dh/dl, assuming laminar flow is obtained using the Hagen-Poiseuille law, Equation 2.2, (see, e.g. Verruijt, 1970 and de Marsily, 1986). The parameters used are the fluid density, ρ, earth acceleration, g, and the fluid dynamic viscosity, μ.

$$Q = -\frac{dh}{dl} \cdot \frac{\rho \cdot g}{\mu} \cdot \frac{\pi \cdot d^4}{128} \tag{2.2}$$

2.4 Conductance in a channel

According to Gustafson (2009) the flow in a channel can be expressed by using the conductance, C, and its hydraulic gradient, dh/dl, as in Equation 2.3. Where the conductance, C, is equal to the hydraulic conductivity, K, multiplied by the area of the cross-section of the flow, A.

$$Q = -\frac{dh}{dl} \cdot C = -\frac{dh}{dl} \cdot K \cdot A \tag{2.3}$$

When a channel of varying cross-section is taken into account, the flow through it can be considered to be the flow through a series of blocks containing different hydraulic conductivities (Matheron, 1967, see de Marsily, 1986), as shown in Figure 2.2.
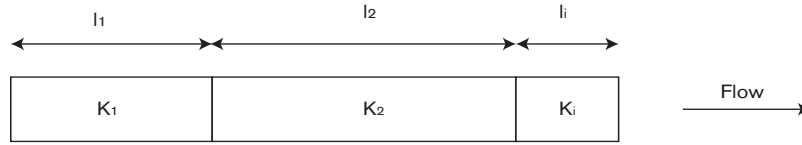

Figure 2.2   *Flow through blocks in series with differing hydraulic conductivity, modified from de Marsily (1986).*

According to the same author, (de Marsily, 1986), the effective hydraulic conductivity in a channel with a varying aperture in series follows a law of harmonic composition where l_i is the length of every block, l_{tot} is the total length, and K_i is the hydraulic conductivity in every block, see Equation 2.4.

$$\frac{1}{K_{harmonic}} = \frac{1}{l_{tot}} \sum \frac{l_i}{K_i} \tag{2.4}$$

2.5   Fracture network and connectivity description

A comparison of the three most common modelling approaches of groundwater flow in fractured rock can be found in Selroos et al., (2002), i.e., Discrete fracture network (DFN), stochastic continuum (SC) and channel network models. All these models calculate the flow in a fracture system composed of several more or less interconnected fractures with different characteristics. The flow in a fracture network will thus not only depend on the transmissivity of every fracture, but also on the orientation, size, frequency and connectivity of the fractures (Selroos et al., 2002).

DFN models, developed by, among others, Andersson and Dverstorp (1987) and Dverstorp and Andersson (1989), assume negligible rock matrix flow and groundwater flows mainly through a network of open fractures with uniform transmissivities. In DFN models, fractures are assumed to be circular discs of arbitrary size, orientation, transmissivity and location, see Figure 2.3a. These models are often used to calculate flow and transport in assumed homogeneous formations, although they do not take into consideration the variation in the fracture aperture within the fracture (Tsang and Neretnieks, 1998).
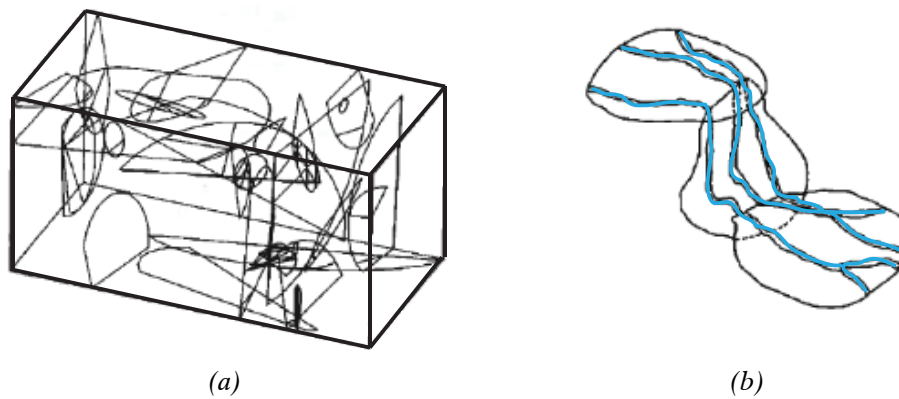
<center>(a)   (b)</center>

Figure 2.3   *Conceptual models: (a) DFN model, modified from Andersson and Dverstorp (1987); (b) Flow channelling through three fractures in series, modified from Tsang et al., (1991).*

The same authors, (Tsang and Neretnieks, 1998), have summarised experimental observations that demonstrate flow channelling in single fractures. According to Tsang and Tsang (1989), flow channelling refers to liquid flow in a heterogeneous fracture structure along a few preferred pathways, where the pathways (paths of least resistance) are where most of the flow goes. Figure 2.3b shows the conceptualised flow in three fractures in series (Tsang et al., 1991).

Furthermore, Black and Barker (2007) shows through a series of brief summaries of experimental observations in underground research laboratories that flow occurring in channels is the dominant flow mechanism rather than some form of sheet flow in planar fractures. The same report suggests that the number of possible channels within a fracture decrease with depth, since the effective stress across fractures increases, gradually closing them.

2.6 Hydraulic tests

A water pressure test (WPT), which is a short-duration test, consists of injecting water into a section, e.g. 3-metre sections of a borehole, or the complete borehole (one section covering the total length) at a specific constant overpressure until the flow, Q, has reached a quasi-steady state condition (few minutes). Natural inflow tests (NITs) on the other hand, do not inject water through the borehole. It is kept open and the measured flow, Q, is driven by the groundwater head. Among others, Houlsby (1990) and Kutzner (1996) describe in detail hydraulic tests such as WPTs. Since no significant time and no special equipment is needed, a WPT is the most common test used during grouting operations to evaluate the

transmissivity, and has been used as the main test in the different projects presented in this thesis.

As shown in Figure 2.1, the aperture of a fracture varies, which is difficult to determine *in situ*, along the longitudinal section, influencing the rock mass permeability. An alternative approach therefore is to use short-duration hydraulic tests, such as WPTs, where the specific capacity (*Q/dh*) is approximately equal to the transmissivity, *T*, (Fransson, 2001). In this test, *Q* is the flow of water into or from a borehole section and *dh* is the driving hydraulic head. Using the evaluated hydraulic transmissivity ($T \approx Q/dh$) and the cubic law, Equation 2.1, the hydraulic aperture, *b*, can be calculated.

2.7 Variogram function (rate of transmissivity change) and kriging interpolation (transmissivity fields)

According to Myers (1997) and Kitanidis (1997) among others, a (semi-) variogram function (*γ(h)*) may be defined as Equation 2.5 where *N(h)* denotes the set of pairs of observations and *h* the lag distance. This means that the variogram shows the variation between pairs of data as a function of the distance between them. The variable *Z(x)* in a grouting operation is considered to be the transmissivities calculated from WPTs in a logarithmic form to facilitate the calculation.

$$\gamma(h) = \frac{1}{2 \cdot N(h)} \sum_{i=1}^{N} \left[Z(x-h) \right]^2 \qquad (2.5)$$

Using the logarithm of the transmissivities obtained from WPTs and the borehole co-ordinates, an experimental variogram can be established and a model variogram can be fitted. As an example, a theoretical spherical variogram model is presented in Figure 2.4, where the sill and range are shown. The resulting graph will show the spatial continuity or roughness of the analysed transmissivity data represented by the range, and the interpreted correlation length signifies that there is no correlation between points further apart than that distance. This can be seen as a measure of the conductive areas or patches in the fractures.

Furthermore, this procedure can be used before grouting in order to investigate the length of the conductive patches and after grouting to see if these patches remain. The rate of transmissivity change along a specific orientation can thus be obtained by the variance, which is provided by a variogram. A similar technique

was used by Hakami and Larsson (1996) to calculate the spatial correlation in a specimen of a single natural fracture. Larsson and Zetterlund (2004) used a variogram analysis to predict the radius of influence of control boreholes in a tunnel after grouting.
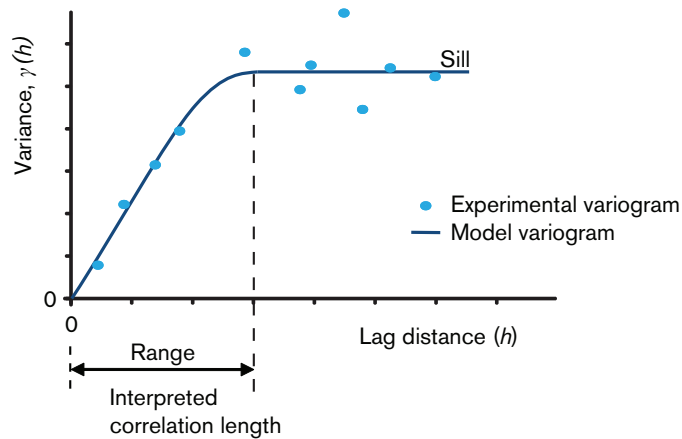

Figure 2.4   Example of a theoretical spherical variogram model fit to an experimental variogram (Myers, 1997). The sill, range and nugget are shown.

The variogram model obtained can be used for spatial interpolation by kriging in the same orientation as the variogram (de Marsily, 1986, and Kitanidis, 1997, among others). This results in a graph showing the interpolated transmissivity across the rock mass surrounding the planned tunnel contour, "the transmissivity field".

Hence, the transmissivity field is an interpreted visualisation of where, in the rock mass, there are transmissive fractures and where the rock is tight. This analysis can be done before and after grouting and consequently the transmissivity reduction effects caused by the grouting process can be visualised using this method. When interpreting a kriging diagram it must be borne in mind that it does not show a true cross-section of the rock mass as the input data come from the whole length of the tested boreholes.

2.8   Flow regimes and dimensionality

As described by Doe and Geier (1990), the flow regimes that can occur within a rock mass could be classified in one, two or three dimensions. 1D represents flow that moves through channels in a fracture where the area of the cross-section of the flow remains constant; 2D represents flow that moves as a wetting front

advancing at a uniform rate, occupying the whole fracture, or as radial flow in a fracture; and 3D represents spherical flow, which includes several fractures connected in a network. These are illustrated in Figure 2.5. However, 3D flow would be difficult to obtain if the injected volume is small and the fractures intersected by the borehole are few, thus suggesting possible hydraulic fracturing during grouting instead.
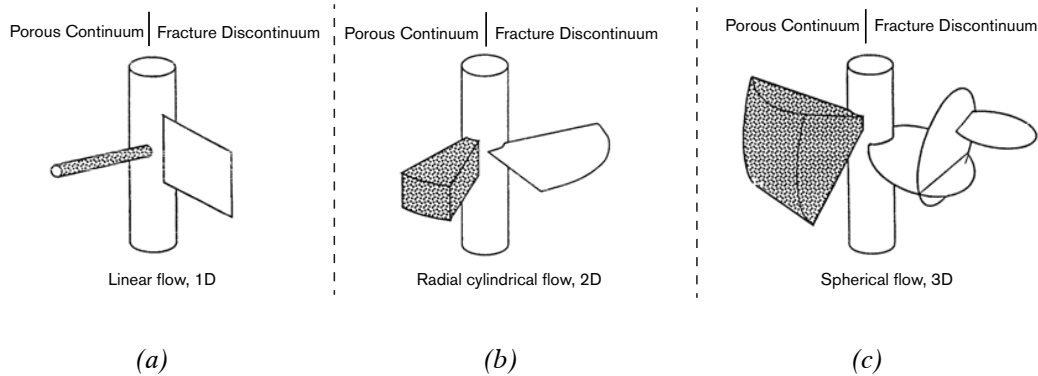

Figure 2.5   *Spatial flow dimensions. In each figure: To the left, flow in porous media, to the right, flow in a fracture; modified from Doe and Geier (1990).*

Follin (1992) has shown through numerical calculations that the flow regime is related to the conductivity variation with regard to different variance analyses. It was also shown that channelling in a low conductive patch seems to be related to the correlation structure, e.g. an uncorrelated field (no correlation length) would contain several minor channels of weak intensity and a correlated field (visible correlation length) would contain one or only a few channels of great intensity.

When the injection of grout during grouting is considered leaving aside the hydraulic tests described previously, Gustafson and Stille (2005) developed an equation, Equation 2.6, that can be used to diagnose the flow regime during grouting. Pressure, volume, time (PVT) recordings during grouting can be obtained and parameters such as momentaneous flow, Q_{mom}, accumulated time, t, and accumulated volume, V, can be evaluated for diagnosis of the flow dimensionality.

$$\frac{d \log V}{d \log t} = \frac{Q_{mom} \cdot t}{V} \tag{2.6}$$

Table 2.1 shows three possible approximate indicator parameters ($Q_{mom} \cdot t/V$) as well as their denotation to which flow regime they correspond and what they

represent. According to Gustafson (2007), these values can be used for colloidal silica in the same way as for cementitious grouts. Special attention must be given to $Q_{mom}{\cdot}t/V$ values higher than 1 since, apart from theoretically meaning a 3D flow, it could also mean that hydraulic fracturing during grouting has occurred.

Table 2.1   *Slope value and flow regime denotation. An approximated value higher than 1 could be expected for a 3-D flow regime or hydraulic fracturing during grouting.*

$Q_{mom}{\cdot}t/V$ (approximate value)	Flow regime	Denotes
0.45	1D	Channelled flow
0.8	2D	Advancing wetting front or Radial flow
1 or higher	3D	Spherical flow, or possible Hydraulic fracturing during grouting

2.9   Unsaturated flow

Description

Single-phase flow is best described as the flow of one kind of matter as a solid, single-phase liquid or gas without any combination, see, for example, Kleinstreuer (2003). Saturated groundwater flow is quite well known and its assumption is quite convenient when attempting to understand basic fracture flow processes and obtaining different parameters that are important to characterise the rock mass for grouting purposes.

On the other hand, Kleinstreuer (2003) describes two-phase flow as the flow of two different kinds of matter, e.g., gas bubbles in liquid, solid particles in liquid, or droplets in gas, where the phases are separated by interfaces. Fortunately, in an underground excavation the two most common substances flowing through the permeable fractures are water and air, and unsaturated flow is thus focused on this interaction and possible multiphase problems are not studied further due to their high complexity and lack of relevance.

Unsaturated flow in porous media

In porous media, during the drainage of saturated pores air starts to intrude into the largest pores, as the capillary pressure, *Pc*, in these pores is the lowest (largest pores drain first); and water will thus flow through tortuous paths in the smaller pores (Rasmuson, 1978). The capillary pressure is therefore a function of the degree of saturation, as shown in Figure 2.6, (see, e.g., de Marsily, 1986). This figure shows the hysteresis effect when the porous media is drained or wetted.
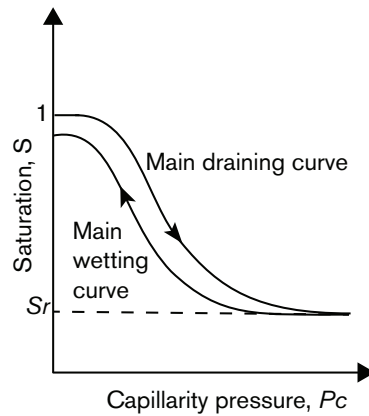
Figure 2.6   *Idealised curve showing the relationships between the degree of saturation, S, and capillarity pressure, Pc, in porous media. Draining and wetting curves, modified from Larsson (1997);*

The result of unsaturated flow in a porous media is that the hydraulic conductivity, *K*, will decrease (sharp drop initially followed by a more gradual decline) as the volume of pore occupied by water decreases (Larsson, 1997), see Figure 2.7a. If the water content starts to increase instead (main wetting curve) a hysteresis effect is observed, see Figure 2.7a, and two possible curves can thus be obtained. This highlights the importance of knowledge of the prior moisture history of the sample (Fetter, 2001).
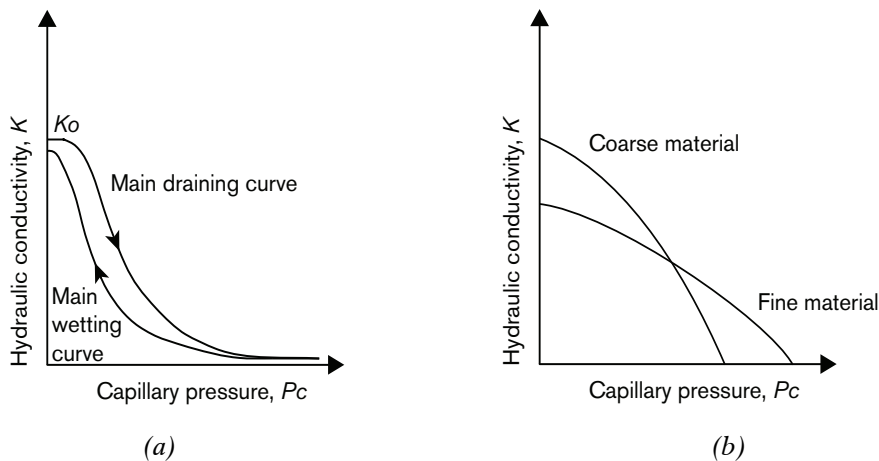

Figure 2.7   *Idealised curves showing relationships between hydraulic conductivity, K, and capillarity pressure, Pc, in porous media: (a) Draining and wetting curves, modified from Larsson (1997); (b) Crossover effect for coarse and fine material, modified from Fetter (2001).*

An important aspect in unsaturated flow, explained by Fetter (2001), is that the hydraulic conductivity depends on the size of the pores. Figure 2.7b shows that at lower water content (high capillary pressure) coarse materials have a lower hydraulic conductivity than fine materials.

The flow of water in unsaturated porous media is represented by Equation 2.7, which is a combination of Darcy's law and the continuity equation suggested by Buckingham. This flow equation in a transient state was developed by Richards (1931) see (Dingman, 2002). The parameters used are the hydraulic conductivity, K, the pressure head, ψ, the elevation above a vertical datum, z, the water content, θ, and time, t, when the transient state is studied.

$$Q = -K(\theta)\frac{\partial h(\theta)}{\partial z} = -K(\theta)\left(1+\frac{\partial \psi(\theta)}{\partial z}\right) \tag{2.7}$$

Unsaturated flow in fractures

In a similar manner to porous media, rock fractures within the periphery of a tunnel will be drained by gravity (wide fractures or open areas in a fracture), if the recharge is not enough to keep the system saturated, and in others (narrow fractures or closed areas in a fracture) water will be bound by capillary forces.

Consequently, in unsaturated conditions the transmissivity of a fracture with a variable aperture is no longer constant; it decreases according to the degree of saturation. This is supported by Jarsjö and Destouni (1998) model results, which indicate that the transmissivity of a system of interconnected fractures with different aperture characteristics decreases due to accumulation of gas in some of the fractures. The transmissivity of the remaining connected fractures does not change and prevents pressure build-up and gas re-dissolution in the interconnected fractures where the transmissivity was reduced. Unsaturated flow processes have been studied, among others by Persoff and Pruess (1995), Geller et al. (1996) and Geller et al. (1997).

Unsaturated flow in rock fractures has been observed through research in relation to nuclear waste storage for a conceptual disposal of nuclear waste where the repository was intended to be situated in a fractured tuff above the water table (Wang and Bodvarsson, 2002). SKB has also funded research into this problem (e.g., Larsson, 1982, Gnirk and Gray, 1992, and Jarsjö et al., 2001). This means that the unsaturated flow will cause the inflowing water to be linked from the wider fractures to the thinner ones and to channels. In principle, the flow direction will be the same as in grouting, where grout penetrates the most

conductive patches first and the connecting channels later. Bockgård and Niemi (2004) have observed formation of local unsaturated zones below the groundwater table when modelling groundwater flow at high gradients in heterogeneous fractured rock covered by a soil layer.

Geller et al., (1997) created a transparent fracture replica that had a variable aperture and dyed water was supplied to the top of the replica with variably saturated flow conditions. Two main paths were created and water moved along with some temporal variations, although fairly stable over time. Cycles of draining and filling were observed even when constant pressure boundaries were used. In their experiments, the angle of the replica could be changed, which allowed the strength of capillarity and gravity forces to be varied.

In laboratory experiments, Persoff and Pruess (1995) observed instabilities with pressure fluctuations even under constant boundary conditions. The instabilities were the result of the interplay between the capillarity and pressure drop. This could be of great significance to the dripping process observed after excavation, which means that the movement of dripping spots along a fracture could be the result of unsaturated flow where different paths are created in which water moves and drips with some temporal variations.

3   CONCEPTUAL MODEL

This chapter presents a hypothesis of the conceptual models of the conductive fracture system before and after excavation. These models aim to provide an understanding of the groundwater conditions in and close to the tunnel roof where dripping takes place. The alternative paths for water to ingress into the tunnel according to the different grouting design concepts are also explained in this chapter.

3.1   Before excavation and grouting

A conceptual model of the conductive fracture system needs to be addressed as a starting point in order to understand the inflow processes in and close to the tunnel roof where dripping takes place before excavation. An analysis of the results from WPTs and PVT recordings made during grouting in the Nygård Tunnel thus made it possible to develop a hypothesis of the conceptual model of the conductive fracture system.

This conceptual model shows how the conductive structures in the rock mass around the tunnel contour are supposed to be linked, see Figure 3.1. As a result, a combination of a variogram, kriging interpolation and dimensionality analysis would provide a deeper understanding of the heterogeneity and connectivity of the rock studied. The conductive fracture system is assumed to be composed of fractures with transmissive patches (2D-flow fractures) connected by less-pervious channels (1D-flow fractures), see Sections 6.1 and 6.2.
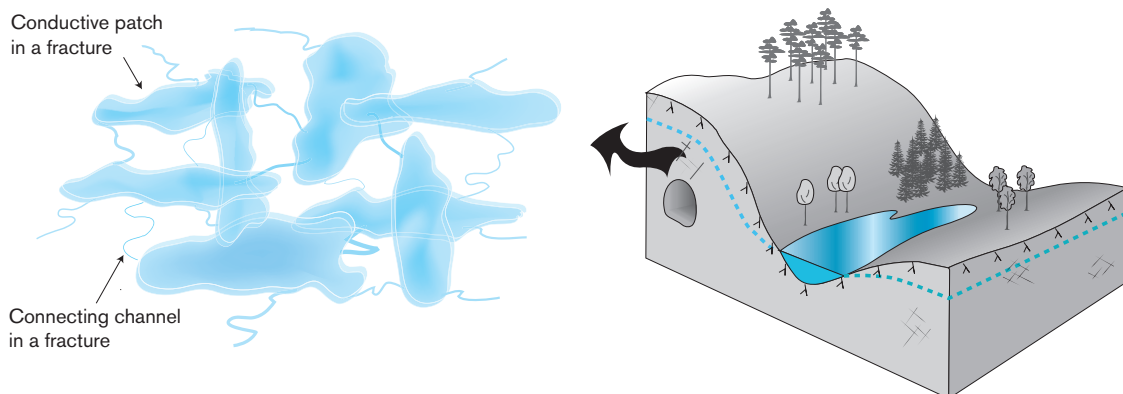

Figure 3.1   Conceptual model of the conductive fracture system before the excavation of a tunnel in a crystalline fractured rock.

3.2   After excavation of a grouted tunnel

Grouting of the previously conceived fracture system will seal most of the conductive patches that were intersected by the grouting boreholes and thus some of the connected channels. This will leave ungrouted channels and fractures that have an inconvenient orientation and are therefore not intersected by the grouting boreholes, see Section 6.3.

Furthermore, it is thought that these channels and unsealed conductive patches, which are emptied mainly by gravity creating unsaturated conditions, will produce the remaining dripping, see Figure 3.2. This is commonly observed in a tunnel following excavation. The unsaturated condition in the remaining patches is expected to create preferential flow paths, which could be an explanation for the movement and fluctuation of the dripping spots observed over time in the different dripping characterisations, see Sections 6.4.
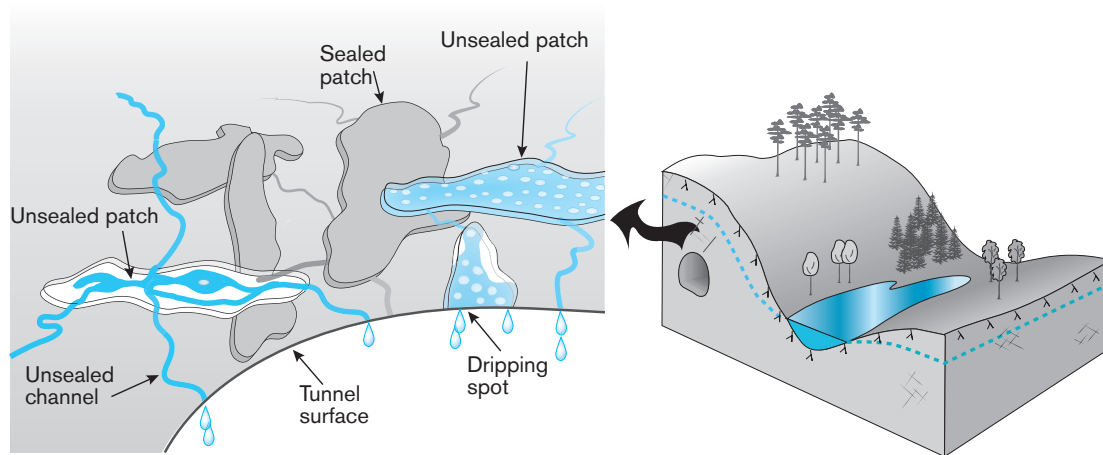
Figure 3.2   *Conceptual model of the conductive fracture system following excavation of a grouted tunnel in a crystalline fractured rock.*

3.3   Hydraulic head implication due to grouting

As an example, a simple numerical calculation of leakage into a section of a non-grouted and a partially grouted tunnel, 35 m^2 in area and situated 20 m below ground, is shown in Figure 3.3. This example assumes the rock to be hydraulically homogeneous, the groundwater level to be at the ground surface (constant head boundary condition) and with increasing pressure with depth.

The flow at each point in the domain is calculated using Darcy´s law, where the groundwater pressure at a point is approximated using the average value of the groundwater pressures in the surrounding cells. A similar modelling approach can be found in Christiansson et al. (2009). The total inflow into the tunnel is obtained by adding the inflows from each leakage point surrounding the tunnel. The total seepage obtained is shown in bars in relative units of $[K \, (m^3/s/m)]$ since no particular value for the hydraulic conductivity, K, was assumed. Figure 3.3a indicates that in a non-grouted tunnel most of the groundwater will flow in at floor level and at the lower part of the walls.

Inflows into a non-grouted tunnel   Inflows into a partially grouted tunnel

(a)   *(b)*
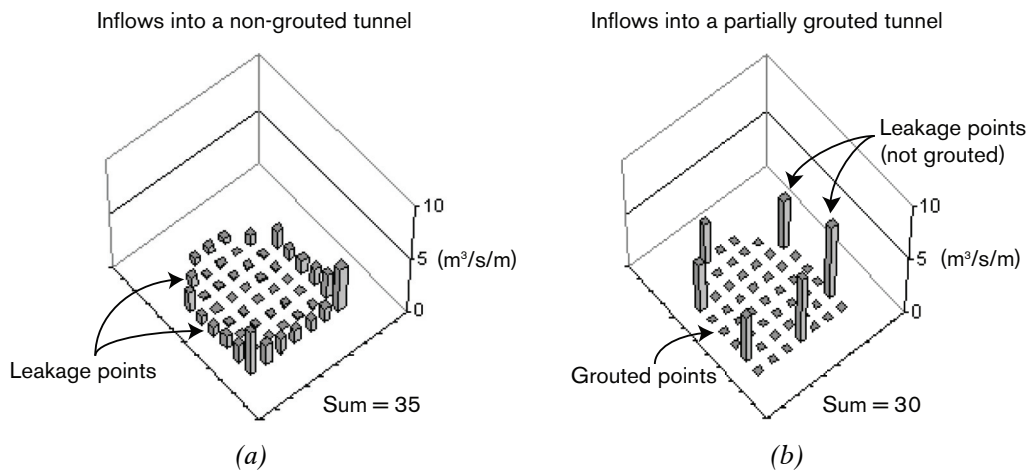
Figure 3.3   *Estimated inflows around a tunnel periphery: a) Inflow into a non-grouted tunnel; b) Inflow into a grouted tunnel where ¾ of the leakage points are sealed.*

On the other hand, Figure 3.3b shows the leakage into the same tunnel, where three-quarters of the leakage points in the tunnel periphery are sealed. A comparison of both figures shows that the total leakage (sum of leakage points) only decreases from 35 to 30 or by 14%. Furthermore, the difference in magnitude between the leakage points becomes smaller, which means that the leakage from the ceiling has increased. The model, as simple as it is, thus confirms the common experience of badly conducted grouting resulting in moving the leakage points rather than decreasing the leakage (Rhén et al., 1997). Comparing this calculation with a real case, we find that the wider fractures are easier to seal, which means that the leakage points will move to the fine fractures, where the leakage will increase. According to Figure 3.3b, this will be most evident in the tunnel roof.

Figure 3.4 shows a schematic illustration of different grouting concepts, where the numbers within the figures represent different grouting agents (1 means cement

and 2 means silica sol) and the broken arrow lines represent the alternative paths for the water to ingress into the tunnel. Assumptions made are that (1) silica sol will greatly reduce the transmissivity of the rock mass where it is used, making it almost impervious and (2) the transmissivity reduction using cement is less than with silica sol since its penetrability is proportional to the fracture aperture (Gustafson and Stille, 2005 and Funehag and Gustafson, 2008b) and narrow fractures will be left unsealed. This difference in transmissivity in the grouting design alternatives used in the different projects covered by this thesis, is expected to produce the illustrated flow paths around the tunnel contour.

In Figure 3.4a a partially grouted tunnel is illustrated and, as explained previously, the leakage points will move to the fine fractures around the tunnel, where the leakage will increase as shown in Figure 3.3b. Groundwater will thus flow into the tunnel at different magnitudes, this will be most evident in the tunnel roof. A second alternative, see Figure 3.4b, illustrates the sealing of the tunnel roof with a material that has good penetration ability and the walls and floor with a material that has less penetration ability. This design is expected to reduce the inflow to satisfy the environmental demands and reduce the transmissivity of the roof to a large extent, redirecting the flow paths to the lower parts of the walls and floor of the tunnel, helping to obtain a drop-free roof. The third alternative, where the inflow demands have already been met and grouting is not required, shows the grouting of the tunnel roof only to waterproof it. This design concept will redirect the inflow into the lower parts of the walls and floor of the tunnel as shown in Figure 3.4c, and again help to obtain a drop-free roof.

(a)   *(b)*   *(c)*
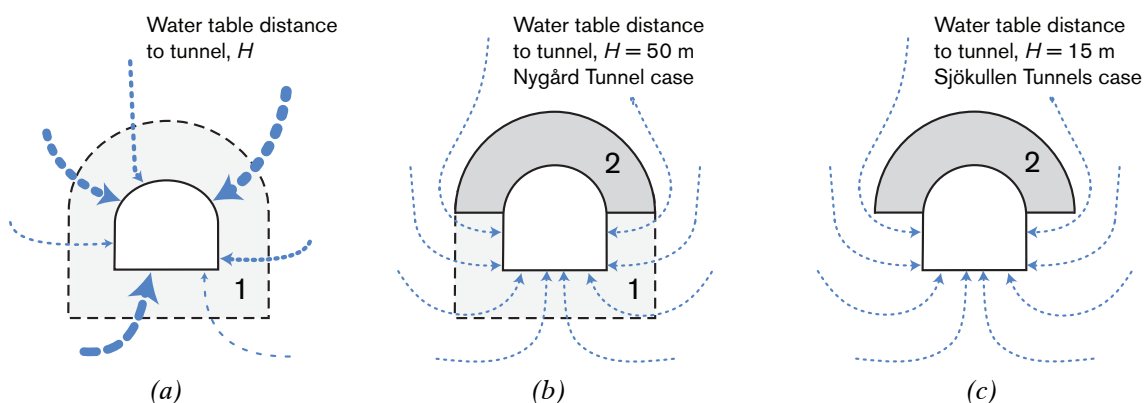
Figure 3.4   *Illustration of the different grouting concepts and flow paths. The number represents different grouting agents and the broken arrow lines the alternative paths for the water to ingress into the tunnel: a) A partially grouted tunnel; b) The roof is grouted with a material that has good penetration ability; the walls and floor are grouted with a material with lower penetration ability (Nygård Tunnel case study); c) The roof is the only area grouted (Sjökullen Tunnels case study).*

4   PUBLICATIONS

In this chapter, a summary of the appended publications is given which includes a brief background, the aims and the main conclusions.

4.1   Publication I: Grouting material tests for drip sealing

A need for a suitable grout to be used in underground constructions where the water tightness requirement is high led to the investigation of silica sol, as cement was not thought to be capable of penetrating the narrow fractures that produce dripping. In addition, some previous investigations suggested that silica sol is a suitable grout to seal narrow fractures (Funehag, 2007 and Funehag and Gustafson, 2008a).

According to Mitchell (1981), cement-based grouts can penetrate and seal fractures that are about three times their particle size. IC 30 (the type of cement commonly used) can thus penetrate fracture apertures larger than approximately 0.1 mm. Silica sol is a refined product of colloidal silica, where the particle sizes have been reduced to between 5 and 100 nm. Laboratory tests were performed to determine the behaviour of silica sol as a permeation grout in crystalline rock.

Results showed that the initial shear strength of silica sol, a few kPa, increases over time. Silica sol demonstrates ductile behaviour during the first few days and then becomes elastic-plastic. Its hydraulic conductivity ranges from 10^{-10} to 10^{-11} m/s. The main conclusions are as follows: (1) The strength obtained in silica sol after hardening is sufficient to withstand the groundwater pressure in most grouting conditions, (2) When sufficiently confined, which is the case for silica sol grouting in rock, silica sol is able to withstand loading and unloading cycles, which means that silica sol is a material that carries a low risk of failure under blasting vibrations, (3) A pH environment of around 11 does not change the strength of the silica sol appreciably, (4) Due to its low hydraulic conductivity, silica sol can be compared to clays with low permeability.

4.2   Publication II: A drip sealing grouting design

The Nygård Tunnel, a double-track railway tunnel, is located in the west of Sweden and is part of the "BanaVäg i Väst" project. It is located 40 to 50 m below ground and is approximately 3 km long. A total of 86 m were tested using a

drip sealing, pre-excavation grouting design concept. The grouting design comprised the use of silica sol in the tunnel roof and cement for the lower parts of the walls and the floor of the tunnel. The excavation, which was performed using drill and blast, went through a sequence of Precambrian gneiss where its foliation dips gently towards the west. The permitted inflow set by the authorities during construction of the tunnel was between 4 and 9 L/min in a 100 m tunnel section.

Five fans in total were grouted and in each of them WPTs were conducted before grouting and after grouting to estimate the achieved reduction in transmissivity. Dripping characterisation was conducted after the tested section was excavated. It is important to state that the grouting design concept assumed that all fractures behave as smooth, parallel plates placed closed together (all fractures have 2D-flow).

The main conclusions are as follow: (1) The total transmissivity was reduced from $4.9 \cdot 10^{-8}$ m^2/s before grouting, to less than the measurement limit ($1.6 \cdot 10^{-8}$ m^2/s) after grouting, implying that the combination of the grouting materials was suitable to remain below the inflow limit, (2) The dripping was reduced to eight spots, located in three different fans. These spots were then covered by geomembrane lining, representing less than 10% of the grouted area. In the whole tunnel, approximately 31% of the roof and wall area was covered by geomembrane lining. All this indicates that the grouting design was successful since dripping was either reduced or prevented and the total transmissivity was reduced, thus reducing the total inflow into the tunnel. In the tested section, few geomembrane lining were used to control the located dripping spots.

4.3   Publication III: Conceptual model development

A conceptual model of the fracture system, consisting of a combination of fractures with 2D-flow and channels with 1D-flow, was developed in this publication with data from the Nygård Tunnel project. The aim of this study was to characterise the rock using data from a pre-excavation grouting experiment for drip sealing purposes. The scope of work was to measure and collect data from WPTs before and after every grouting operation, analyse the hydraulic homogeneity and conductivity of the rock by variogram analyses and assess the transmissivity field of the rock mass in every fan by means of a kriging interpolation of the borehole transmissivities.

Results show how the WPT data can be used to assess the characteristic size of the conductive patches in fractures before grouting and the very limited or even lack of correlation of the remaining unsealed channels after grouting. The main conclusions are: (1) There is a system of conductive patches dispersed in a less pervious rock, which can be interpreted as transmissive fractures. Although their size complies with the size of the major water-bearing fractures, these patches are smaller than the longest observed fractures and the patch size would thus be the size of the open transmissive areas in a fracture and not their total length. The system of conductive patches is relatively easy to intersect and fill with grout provided the aperture is sufficiently large for penetration; (2) This conductivity system is connected by a network of less pervious channels, which constitute low permeability connections between the conductive patches. These channels could be the intersection of two narrow fractures or a channel system in a low conductivity fracture with large contact area or large filling areas in an open fracture. These channels are difficult to intersect by a borehole and are thus difficult to grout; (3) All these findings support a conceptual model of the rock mass around the tunnel contour as a system of conductive patches connected by much less conductive channels.

4.4 Publication IV: Licentiate thesis

Apart from the literature study, the licentiate thesis links some of the early findings with the problems stated at the beginning of the project and provides a basis for further research. This means that the conceptual model was addressed but not verified, and an analysis of how the remaining dripping influences the risk of ice growth and icicle formation during winter was made and can be explored in detail in Butrón (2009).

The main conclusions of the licentiate thesis are as follows: (1) The pre-excavation grouting design in the Nygård study case reduced the leakage to the permitted inflows and minimised the dripping, (2) A first conceptual model of the fracture system was addressed. This was composed of a combination of conductive patches connected by less conductive channels, (3) The temperature conditions did not seem to give rise to a risk of ice growth, (4) Since geomembrane lining was used, icicles are not expected to occur from the covered dripping spots, although ice accumulation between the rock and the geomembrane lining could be possible.

4.5   Publications V and VI: Corroboration of the conceptual model

At the Äspö Hard Rock Laboratory a test tunnel was constructed between 2007 and 2009 – the TASS Tunnel. It is located 450 m below ground and the main rock type is diorite. One of the aims of the project was to control the inflow by means of pre-excavation grouting and, if necessary, post-excavation grouting. WPTs and other hydraulic tests were conducted in each borehole before and after the pre-excavation grouting of each fan.

The aim of Publication V was to obtain information about the hydraulic structure of this type of rock. The grouting design and evaluation of the TASS Tunnel is not part of this work and can be explored in detail in (Funehag, 2008) and (Funehag and Emmelin, 2011). The scope of work was similar to that in Publication III: collect data from WPTs before and after each grouting operation, analyse the hydraulic homogeneity and conductivity of the rock using variogram analyses and assess the transmissivity field of the rock mass in each fan by means of a kriging interpolation of the transmissivities of the boreholes.

The main results and conclusions of Publication V are: (1) For the whole tunnel, the connectivity range of the rock before grouting is approximately 3 m, which is similar to the Nygård case in Publication III, (2) The connectivity range is reduced after grouting, which is inferred by the large reduction in the correlation length, (3) The grouting has reduced the transmissivity in the rock by around four orders of magnitude within the studied rock volume of a fan, (4) Results clearly show that the most conductive parts of each fan were where the grout has penetrated the most. This means that a few conductive fractures contribute most to the borehole injection and what is left unsealed after grouting is a highly channelised system. This channelised system will be extremely difficult to intersect with future boreholes, which will make post-grouting a complex task.

The aim in Publication VI is to identify a relevant set of parameters to create a conceptual model of the water-bearing fracture system in a project. This conceptual model is not focused on the structures that produce dripping from the tunnel roof. The difference compared to the analysis made in the previous publication is that the section analysed in Publication VI (one fan) is influenced mainly by a fracture zone while Publication V analyses the whole tunnel (5 fans). WPT data from a 20 m section of the TASS Tunnel was used and the hydraulic structure around the tunnel section where dripping takes place was obtained.

The main results and conclusions concerning the variogram analysis, kriging interpolation and dimensionality analysis are: (1) The correlation length in the 20 m section is approximately 8 m, which supports the existence and importance of the fracture zone intersecting the rock mass if compared to 3 m when the whole tunnel is analysed, (2) The correlation length after grouting is less than 1 m, which again shows that what is left after grouting are channels, (3) The variogram, kriging and dimensionality analyses suggest that a fracture zone can be made up more homogeneously of fractures with mainly 2D-flow, which means that the grouting will be more effective.

4.6 Publication VII: Analysis of the remaining dripping

This study covers the measurement and analysis of the remaining dripping in the previously described TASS Tunnel. One of the aims of the TASS Tunnel project was to control the inflow by means of pre-excavation grouting and, if necessary, post-excavation grouting. The maximum permissible inflow value set for this project was 1 L/min per 60 m tunnel, giving much more attention to the dripping inflow than in standard structural tunnels. In this study, the grouted tunnel was divided into four sections for drip-characterisation.

Results showed that in section 33.8 to 50 m, post-excavation grouting was conducted and the total dripping was reduced from 21 to 8 mL/min per 60 m (June 2009). The main conclusions are: (1) Assuming the pre-excavation grouting sealed to a certain extent all fractures crossing the tunnel, since the tunnel orientation was perpendicular to the main rock stresses giving potentially open fractures that were easy to intersect with the grouting boreholes, parallel fractures and channels in fracture planes not intersected with the grouting boreholes may have been left unsealed. This was confirmed by the drip mapping and the transmissivity fields; (2) Although the post-excavation grouting in section 33.8 to 50 m aimed to seal the fractures that remained unsealed by the pre-excavation grouting, dripping remained after grouting. This indicates that there are structures that were left unsealed.

Christian Butrón

5 FIELD APPLICATION AND OBSERVATIONS

The different grouting design approaches and their evaluations are presented in this chapter. Practical issues encountered during grouting are not included. Two case studies are covered where a drip sealing design was used: the Nygård Tunnel and the Sjökullen Tunnels. One case study, the TASS Tunnel, shows mainly the dripping characterisation conducted after the different grouting stages. The entire grouting procedure in the TASS Tunnel can be explored in detail in Funehag (2008) and Funehag and Emmelin (2011). It is important to state that for the grouting designs all fractures are assumed to behave as smooth, parallel plates with 2D-flow.

5.1 The Nygård Tunnel case study

The Nygård Tunnel case study, which is mostly based on Publication II (Butrón et al., 2010), is located in the west of Sweden and is part of the "BanaVäg i Väst" project, see Figure 1.2. The Nygård Tunnel is located 40 to 50 m below ground and is approximately 3 km long. A total of 86 m were tested, see Figure 5.1. This tunnel consists of one main tunnel and one service tunnel, excavated using drill and blast through a sequence of Precambrian gneiss where its foliation dips gently to the west. The investigation consisted of the design, follow-up and evaluation of the grouting procedure and aimed to reduce the inflow and prevent dripping.
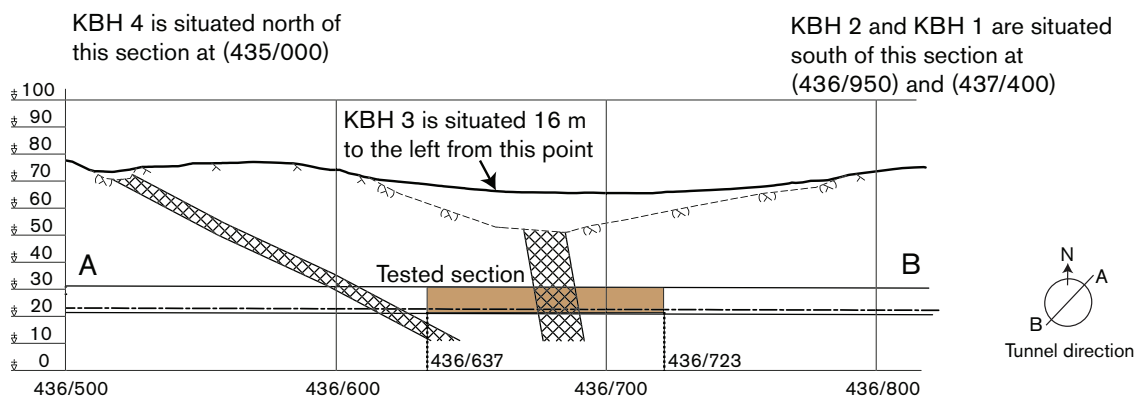

Figure 5.1   Profile illustration and location of the tested section in the Nygård Tunnel, modified from the construction drawings: © Banverket (2005), Norway/Vänernbanan, Torbacken-Hede section.

Pre-investigations

Fracture mapping was conducted from four boreholes (KBH 1 to 4) located along the tunnel line and drilled at different directions and angles to the ground, see Figure 5.1. This fracture mapping consisted of counting the total number of fractures at each 3-metre interval in each borehole. Figure 5.2a shows the number of fractures or the fracture frequency in each borehole, put together in 33 sections. An analysis of the four pre-investigation boreholes gave an average fracture intensity of $P_{10} = 4.1$ fractures/m. WPTs (carried out with the use of packers in each 3-metre section) were conducted in each borehole and the specific capacity, which is assumed to be equal to the transmissivity in the 3-metre sections, was evaluated.
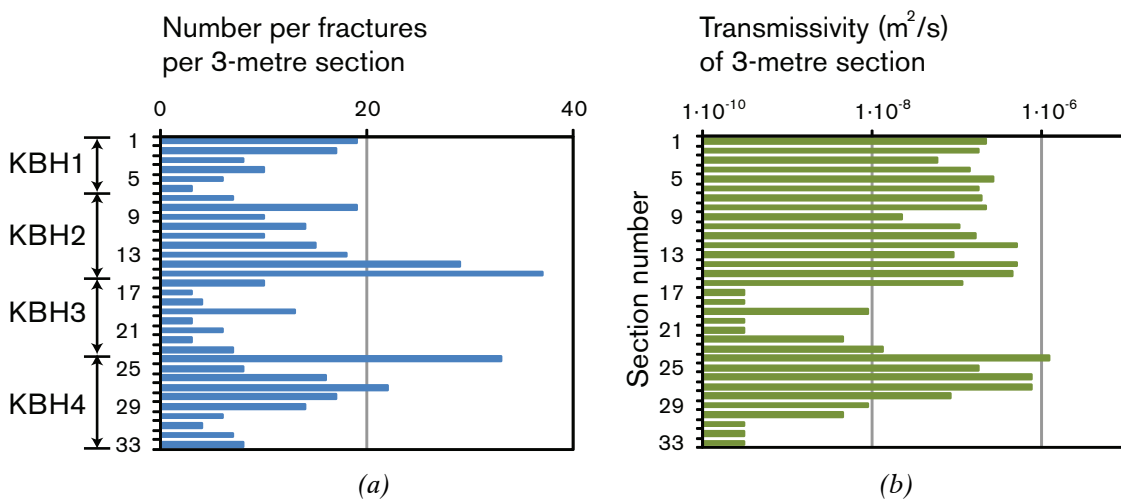

Figure 5.2　　*Data gathered from four pre-investigation boreholes. Each section is 3 m and the number of sections varies in each borehole, Publication II: (a) Fracture frequency per 3 m section; (b) Calculated transmissivities per 3 m section (T ≈ Q/dh).*

The corresponding evaluated transmissivity, assuming 50 m of hydraulic head above the tunnel, is presented in Figure 5.2b. The first section in each borehole was excluded since a noticeably fractured, permeable surface layer was observed. It is not used for the results or for the analysis.

Fracture transmissivity and fracture aperture distribution

Using the fracture frequency and the calculated transmissivities in the pre-investigation stage, a Pareto or power-law distribution was obtained. The Pareto distribution is then approximated as a straight line in a log-log plot after various iterations using the Newton-Rhapson iteration method, see Figure 5.3a.
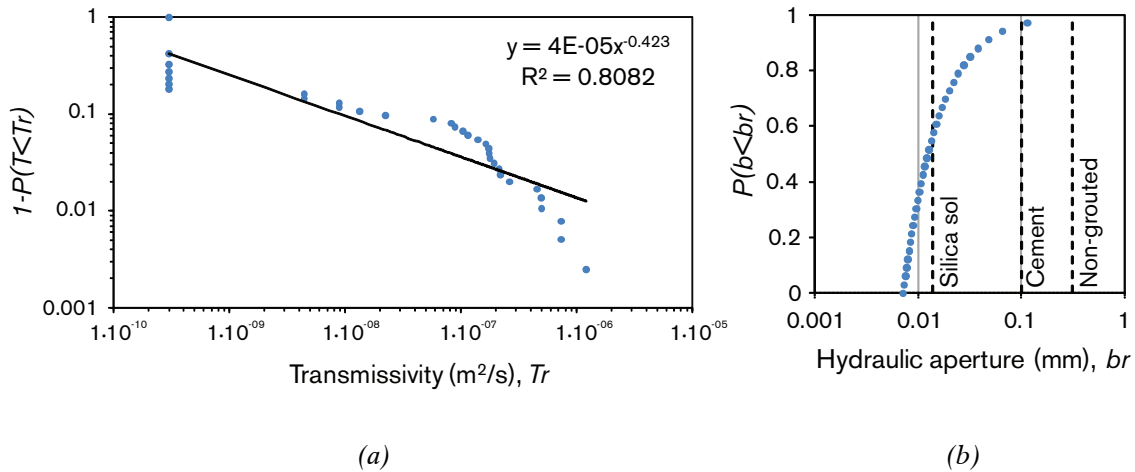
(a)   (b)

Figure 5.3   *Evaluation of data from all four pre-investigation boreholes, see Publication II:*
                 (a) Evaluated Pareto distribution from transmissivities per 3 m section;
                 (b) Calculated hydraulic aperture distribution.

This line has a slope or coefficient of the distribution (-k) equal to 0.423. All these steps are well explained in Butrón et al. (2010). Gustafson and Fransson (2005) describe the method of obtaining such a distribution in more detail. Subsequently, the cubic law presented in Equation 2.1 can be rearranged in a way that the hydraulic aperture (b) is related to the transmissivity (T) instead and the hydraulic aperture distribution can be estimated.

Figure 5.3b presents the estimated hydraulic aperture distribution using the cubic law and the Pareto distribution coefficient (-k) obtained previously, see Gustafson and Fransson, (2005). As can be seen in Figure 5.3b, around 97% of the fractures have a hydraulic aperture of less than 0.1 mm and around 60% of them have an aperture of less than 0.014 mm. These limits are used to decide which grout should be used. One observation is that the distribution clearly shows that the major contribution to the transmissivity of the borehole comes from a few wide fractures, se Figure 5.3a.

Grout type and penetration distribution

Butrón et al., (2009) showed that silica sol is a suitable grout for use in a drip sealing grouting procedure due to its low hydraulic conductivity, low risk of failure due to blasting vibrations, capacity to withstand the groundwater pressure in most grouting conditions after hardening and ability to penetrate these narrow fractures that cause small inflows.

According to Funehag (2007) and laboratory studies made by Axelsson and Nilsson (2002), silica sol can penetrate and seal narrow fractures down to approximately 10 to 14 µm, which offers the potential to minimise dripping. On the other hand, according to Mitchell (1981) and Eklund (2005), cementitious grouts can as a rule penetrate and seal fractures that are about three times or more their particle size, around 0.1 mm in this case where IC 30 (type of Portland cement) is used.

For these reasons and in the light of the hydraulic aperture distribution, the tunnel roof was grouted using silica sol in order to prevent dripping and the lower part of the walls and floor of the tunnel were grouted with cement to reduce the total inflow into the tunnel to the permitted level. Using the determined rheology parameters (Butrón et al., 2010) and the equations described to determine the maximum penetration length with cement (Gustafson and Stille, 2005) and silica sol (Funehag, 2007), the grout penetration for 25 min of injection can be calculated for both grouts and for hydraulic apertures, see Table 5.1.

Table 5.1   *Grout penetration calculated during injection into a fracture (2D-flow) for 25 min with an applied over-pressure (Δp) of 2.5 MPa (Publication II).*

	Hydraulic aperture [mm]	Penetration [m] in a fracture (2D-flow)
Cement	0.1	7
Silica sol	0.014	1.8

Inflow prognosis

The permitted inflow during construction of the tunnel, as stipulated by the authorities, was between 4 and 9 L/min in a 100 m tunnel section. Table 5.2 shows the residual inflows and transmissivities calculated from the combination of unsealed fractures. Since the residual inflow after using cement is 9 L/min in 100 m and the use of silica sol is 2.3 L/min in 100 m, it should be adequate to use a combination of silica sol in the tunnel roof and cement in the floor and walls to control the maximum permitted water inflow into the tunnel.

Table 5.2   *Calculated residual inflows and residual transmissivities after grouting different minimum hydraulic apertures (Publication II).*

Minimum hydraulic aperture sealed [mm]	Residual inflow [L/min·100 m]	Residual transmissivity [m²/s]	Remarks
0.12	9.2	$6.2 \cdot 10^{-6}$	Non-grouted tunnel
0.10	9.0	$4.3 \cdot 10^{-6}$	Grouted with cement
0.014	2.3	$7.6 \cdot 10^{-8}$	Grouted with silica sol

Once colloidal silica is used in the roof, it can be seen that few unsealed fractures (smaller than 0.014 mm in hydraulic aperture) will be left, see Table 5.2, reducing the inflow from the tunnel roof to 2.3 L/min in a 100 m tunnel section, corresponding to an approximate transmissivity of $7.6 \cdot 10^{-8}$ m^2/s. This calculation assumes that the groundwater level is close to the ground surface and that no substantial lowering of it is caused by the construction of the tunnel. Assumptions and equations needed for this calculation can be explored in Gustafson (2009).

Layout and protocol

Since conventional grouting with cement was already being used before incorporation of the drip sealing concept in the Nygård project, the fan layout was the only thing retained to facilitate the continued construction. The layout was also used as input to calculate the penetration length of grout with an overlap of at least 100% between boreholes, see Figure 5.4. This layout follows the concept previously explained in Section 3.3.
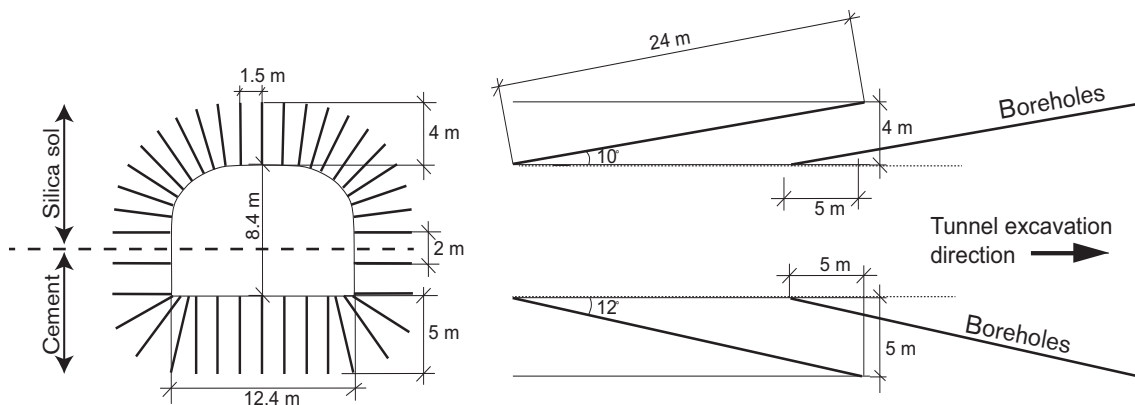

Figure 5.4   Layout of the grouting boreholes for each fan in the tunnel, modified from the construction drawings: © Banverket (2005), Norway/Vänernbanan, Torbacken–Hede section. Front view and lateral view of a cut made in the middle.

The grouting protocol for the Nygård Tunnel, which covered 86 m, divided into five fans, is summarised in Table 5.3, where 20 boreholes located in the tunnel roof were grouted with silica sol and 20 in the walls and floor were grouted with cement. In the end, the resulting fieldwork was kept similar to the suggested protocol. After grouting, around ten control boreholes were drilled in each fan. These boreholes were located next to boreholes that showed high WPT results before grouting or boreholes that took large volumes of grout.

Table 5.3   Summary of the grouting protocol used in each borehole in all fans. All boreholes drilled as control boreholes followed the same procedure, see Publication II.

	Layout	
Number of boreholes per fan	40	
Distance between boreholes (end-point)	1.5 m (roof) 2 m (walls and floor)	
Theoretical grouted zone around the tunnel	5 m	
Overlap between fans	5 m	
Borehole length	24 m	
Borehole diameter	64 mm	
Type of grout	Silica sol	Cement
Minimum fracture aperture to be sealed	14 μm	100 μm
Gelling induction time	13 min	-
Gelling time	40 min	-
Yield strength	-	5 Pa
Density	-	1590 kg/m^3
Marshcone	-	44 s
Pumping over-pressure (Δp)	25 bar	25 bar
Approximate ground water pressure	5 bar	5 bar
Pumping time	21 min	25 min
Minimum calculated penetration length	2 m	7 m

Transmissivity reduction

The results obtained from WPTs conducted before and after grouting showed a reduction in the median transmissivity in the entire tested section from $4.9 \cdot 10^{-8}$ m^2/s to less than the measurement limit ($1.6 \cdot 10^{-8}$ m^2/s), implying that a combination of grouting materials was suitable to remain below the inflow limit, see Figure 5.5b. This suggests that one of the aims was fulfilled.
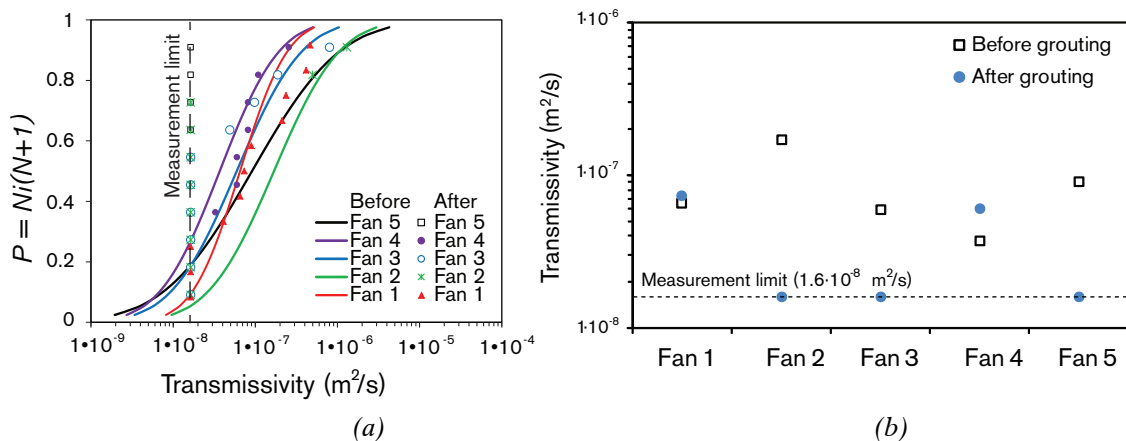

Figure 5.5   Transmissivity values for all fans before and after grouting. The transmissivities are evaluated from 24 m-section boreholes in length, Publication II: (a) Fitted lognormal distribution values in every fan before grouting and measured values without fitting after grouting, (b) Median transmissivity values per fan.

When the results per fan are taken into account, it can be seen that in fans 2, 3 and 5 the transmissivity was reduced to below the measurement limit, fan 4 was quite tight from the beginning and in fan 1 there is no visible reduction, see Figure 5.5a and Figure 5.5b. This is believed to be a consequence of the hydraulic structure of the rock in the tested section, where the rock around fan 1 seems to be composed mostly of channels with low perviousness, limiting the sealing effect and producing most of the dripping spots. This is discussed later in Section 6.5.

Dripping

Figure 5.6 shows the different dripping locations, which were reduced to eight over 86 m, the measured inflow and the location of the geomembrane lining that was eventually placed. The area of the roof and walls in the whole tunnel is 84,840 m^2, which is partially covered by 26,161 m^2 of geomembrane lining (31% of the whole tunnel). The area studied is 2,408 m^2 in total (roof and walls) and geomembrane lining covers 217 m^2, which is less than 10% of the area studied and less than 1% of the total area of the geomembrane lining used (217 m^2 in the studied section divided by 26,161 m^2 in the whole tunnel).

Figure 5.6   *Drip characterisation, showing the location and flow of the localised dripping spots in d/min (drops per minute) and mL/min units are shown. The areas represent the characterisation conducted on September 27, 2008. The assumed hydraulic head is 50 m, Publication II.*

No ice or icicles were formed during the winter of 2008 and 2009, when temperatures remained below freezing. This information was acquired during a visual inspection on March 11, 2009 in the service tunnel and through personal communication (Lindstrom, 2009). The few remaining dripping spots thus indicate that the grouting design was successful since dripping was either minimised or prevented and the total transmissivity was reduced, thus reducing the total inflow. Post-excavation grouting was not needed and few areas with geomembrane lining were used to control the located dripping spots.
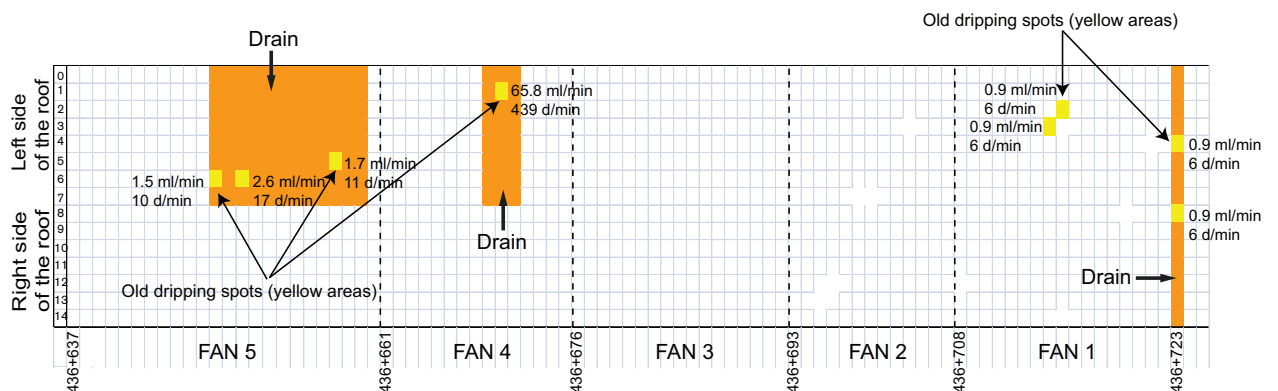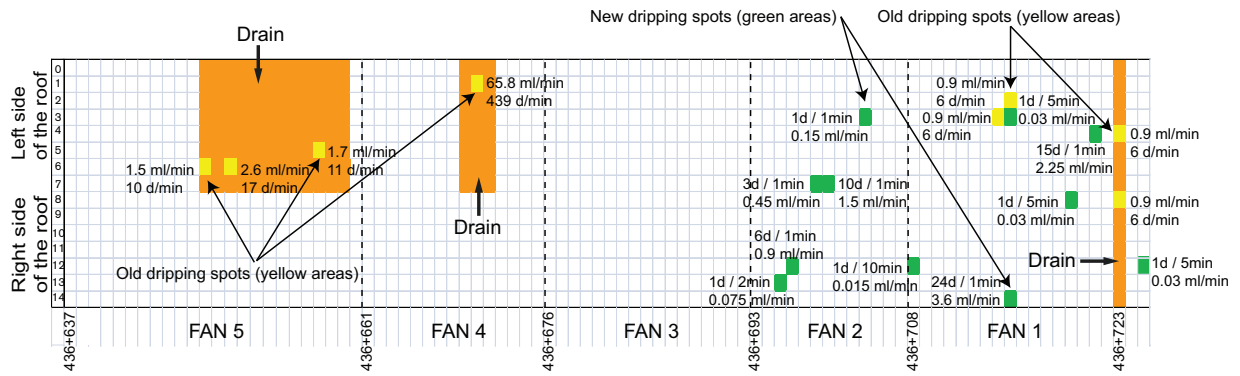
Figure 5.7   *Drip characterisation, showing the location and flow of the localised dripping spots in d/min (drops per minute) and mL/min units are shown. Two characterisations are presented: the yellow represent the characterisation conducted on September 27, 2008, and the green areas represent the characterisation conducted on June 14, 2011. The assumed hydraulic head is 50 m, Publication II.*

A second dripping characterisation, see Figure 5.7, conducted in the same section two years later (June 14, 2011) shows that the newly developed dripping spots are found mainly where fans 1 and 2 were located. The analysis conducted later in Section 6.5 indicates that grouting efficiency depends to a large extent on the heterogeneity of the conductive system of the rock mass. Fan 1, which is composed mostly of 1D-flow structures, offers limited potential for a borehole to intersect and seal all pervious channels, which will produce the new dripping spots. On the other hand, a more homogeneous fracture system, composed mostly of 2D-flow, such as fan 5, means a borehole has a high possibility of intersecting and grouting the open fractures.

5.2   The TASS Tunnel

At the Äspö Hard Rock Laboratory a test tunnel was constructed between 2007 and 2009 – the TASS Tunnel. It is located 450 m below ground and the main rock type is diorite. One of the aims of the project was to control inflow by means of pre-excavation grouting and, if necessary, post-excavation grouting. The maximum permissible inflow figure set for this project was 1 L/min per 60 m tunnel, giving more attention to the dripping inflow than in common structural tunnels. In this study, the grouted tunnel was divided into four grouting stages with a total of seven grouted fans. Extensive information about this project is found in Funehag (2008) and Funehag and Emmelin (2011).

Summary of the pre-investigation results

Based on (Funehag, 2008), a short summary of the pre-investigation results and analysis is presented in this section. Three pre-investigation boreholes, each 100 m long, were used to obtain a Pareto distribution and a hydraulic aperture distribution. This aperture distribution shows a range of apertures ranging from a few to about 200 µm and that all fracture apertures down to around 10 µm must be sealed to meet the requirement of a maximum inflow of 1 L/min per 60 m, which in a way makes the permeation grouting at this site similar to a drip sealing concept. Groundwater pressures were measured at 3.2 to 3.5 MPa. The fracture frequency varied from one fracture to four fractures per metre and also between pre-investigation boreholes.

Summary of the choice of grout and grouting procedure

The choice between using low-pH cement-based grouts or silica sol for each individual borehole was based on the hydraulic aperture distribution. If the inflow from a borehole corresponded to a hydraulic aperture between 0 and 150 µm, silica sol was used, and for 150 µm or larger hydraulic apertures, a low-pH cement-based grout was used (Funehag, 2008).

Table 5.4   Summary of the base grouting protocol used in each fan (Funehag, 2008).

	Layout	
Number of boreholes per fan, valid for the first series of boreholes	Between 20 and 30	
Distance between boreholes (end-point), valid for the first series of boreholes	2 m	
Theoretical grouted zone around the tunnel	4 m	
Overlap between fans	≥ 4 m	
Borehole length, valid for the first series of boreholes	20 m	
Borehole diameter		
Type of grout	Silica sol	Cement (Recipe 1)
Minimum fracture aperture to be sealed	10 µm	150 µm
Gelling induction time	13 or 21 min	-
Gelling time	39 or 63 min	-
Yield strength	-	15 Pa
Viscosity	-	25 mPas
Pumping over-pressure (Δp)	50 or 30 bar	70 bar
Approximate ground water pressure	32 to 35 bar	32 to 35 bar
Pumping time	31 or 50 min	45 min
Minimum calculated penetration length	1.5 m	10 m

The summary of the grouting protocol is shown in Table 5.4. The procedure starts by grouting between three and four 20 m long front holes drilled parallel to the tunnel in order to lower the hydraulic gradient at the tunnel front. Later, three series (A, B and C) of boreholes are grouted, one series at a time, in order to achieve the best sealing outcome possible. Series B and C are used as control boreholes and as a next round of grouting when needed. The distance between the boreholes was adapted to the penetration length calculated for 10 μm and with an overlap of at least 50% (Funehag, 2008).

Dripping characterisation after the pre-excavation grouting

As in the Nygård Tunnel, drip mapping and inflow measurement after the pre-excavation grouting were carried out for each section at different times, following the excavation of the tunnel. Figure 5.8 presents the results from these measurements and the inflow obtained at the monitoring weirs constructed at 10, 33.8 and 50 m. All inflow values at the weirs were measured on June 8, 2009, except for section 33.8 to 50, which was measured on January 5, 2009 (Funehag, 2010).
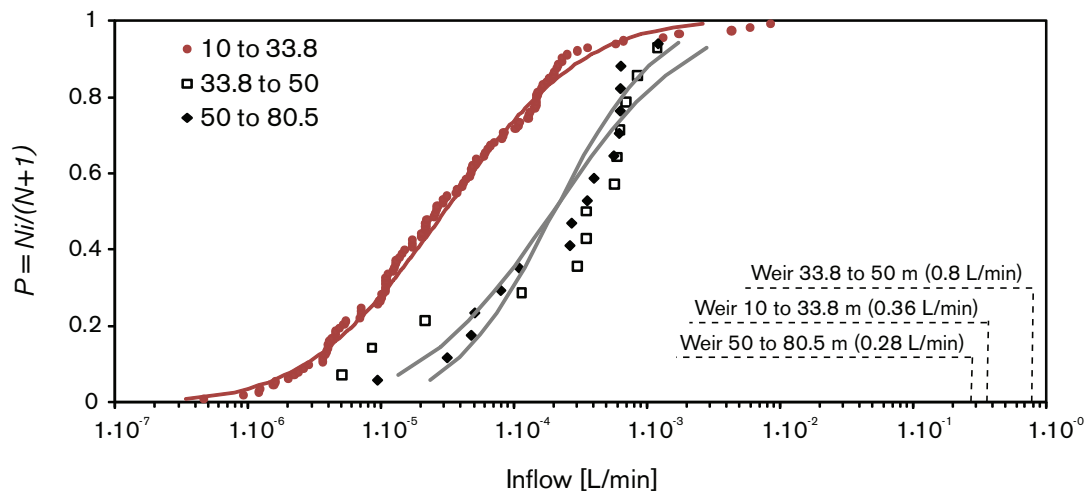

Figure 5.8   *Inflow measurements of the dripping areas characterised in the different sections of the tunnel roof. The fitted lognormal plots are also shown. The inflows obtained at the monitoring weirs constructed at 10, 33.8 and 50 m are shown as dots, Publication VII. The measured hydraulic head is 350 m.*

These plots are close to the lognormal distributions plotted in the same figure and in a way represent the "conductance" found for channelised fractures leading to the roof of the tunnel. This is according to the conceptual model. The pre-excavation grouting sealed to a certain extent all the wide, open fractures

(2D-flow) crossing the tunnel, since the tunnel orientation was perpendicular to the main rock stresses, giving potential shearing fractures that were easy to intersect with the grouting boreholes. Parallel fractures and narrow flow channels in fracture planes were difficult to intersect with the grouting boreholes and may have been left unsealed, resulting in the remaining dripping.

By comparing all the results from the graph it can be seen that two of the three plots show similar results and one is different. This can be explained by the presence of a transmissive fracture zone (Structure 5) in section 10 to 33.8, with an estimated inflow between 25 and 42 L/min (Funehag and Emmelin, 2011), measured in April 2007. This fractured zone seemed to give this section more dripping spots than in the other sections although most of them were simply moist areas.

The different distributions of the dripping results are quite similar in all sections, except for 10 to 33.8, where the fracture zone is located. This implies that in a rock section with no special fracture features and which is quite heterogenic, the sealing effect is similar and thus the residual dripping results. A comparison of the inflows before grouting and the inflow collected in the weirs shows a large reduction in section 10 to 33.8 m, where the fracture zone is located (42 to 0.36 L/min), see Figure 5.8. This implies that the grouting of a rock section that is quite homogeneous the sealing is more efficient. This is discussed in Section 6.3.

Figure 5.8 also shows that the sum of all inflows is considerably lower than the inflows measured at the respective weirs, since the dripping characterisation is a measure of the inflow from the tunnel roof. The rest of the inflow should come from the walls and floor of the tunnel. One reason could be that the water pressures at tunnel floor level are higher than in the roof.

Another possible reason could be that even if no continuous EDZ (no significant axial hydraulic connectivity due to few blast-induced fractures) was found in the TASS Tunnel (Ericsson et al., 2009), a local EDZ located at different locations along the tunnel could allow water to go from the roof to the lower parts of the walls and floor, giving a larger inflow at the floor of the tunnel. Additionally, parallel fractures that were difficult to intersect with the grouting boreholes could have been left unsealed or opened during grouting, which could transport water behind the tunnel wall to the lower parts of the tunnel. This should be investigated further.

Dripping characterisation after the post-excavation grouting

Section 33.8 to 50 m was grouted after being excavated (post-excavation grouting), first in the floor and the walls and then in the roof. The post-excavation grouting reduced the total inflow measured from the dripping spots from around 5.7 mL/min to around 3 mL/min (after the grouting of the floor and walls) and then to around 2.1 mL/min (after the grouting of the roof). This means a reduction in the dripping inflow of approximately 63%. This measured value is far lower than the inflow measured at the weir, 590 mL/min in this section, which means that even after post-excavation grouting most of the inflow comes from the floor and walls of the tunnel.

Figure 5.9 shows the dripping characterisation conducted in the post-grouted section. All the square areas are dripping spots remaining after the post-excavation grouting. In some of these dripping spots the inflow decreased (blue squares) and in some it increased (green squares).

Dripping spots where the inflow increased after the post-excavation grouting of the floor and walls
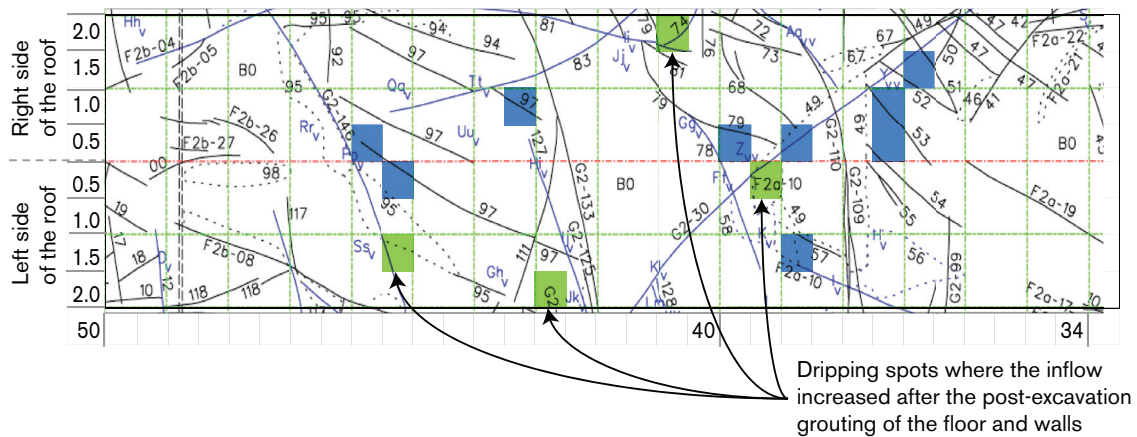
Figure 5.9   Drip and fracture mapping from the tunnel roof in section 33.8 to 50 m. The square areas in the grid represent the measured dripping spots. Lines and dotted lines represent all exposed structures in the tunnel roof according to Sigurdsson (2009).

Assuming that during pre-excavation grouting all fractures crossing the tunnel were sealed to a varying extent, possibly leaving parallel fractures and channels unsealed, which is in accordance with the conceptual model, the post-excavation grouting should have sealed the remaining set of fractures, and what is left should just be isolated narrow fractures and channels. A possible practical implication of this is that further grouting will only seal those very narrow fractures and channels that are crossed by the new boreholes (local grouting) and the remaining bulk conductivity will be reduced only slightly.

5.3   The Sjökullen Tunnels

The Sjökullen Tunnels case study area is in the Municipality of Vänersborg in the west of Sweden and, as with the Nygård Tunnel, they are part of the "BanaVäg i Väst" project (Trafikverket, 2011b). The investigation was conducted in two tunnels, which are situated near a lake, Sjökullesjön. The tunnels are the Sjökullen North Tunnel, see Figure 5.10a, and the Sjökullen South Tunnel, Figure 5.10b, each of which are approximately 120 m long and located 10 to 15 m below ground. These tunnels are 100 m apart (one after the other) which gives a good opportunity to see the results of two different grouting designs.
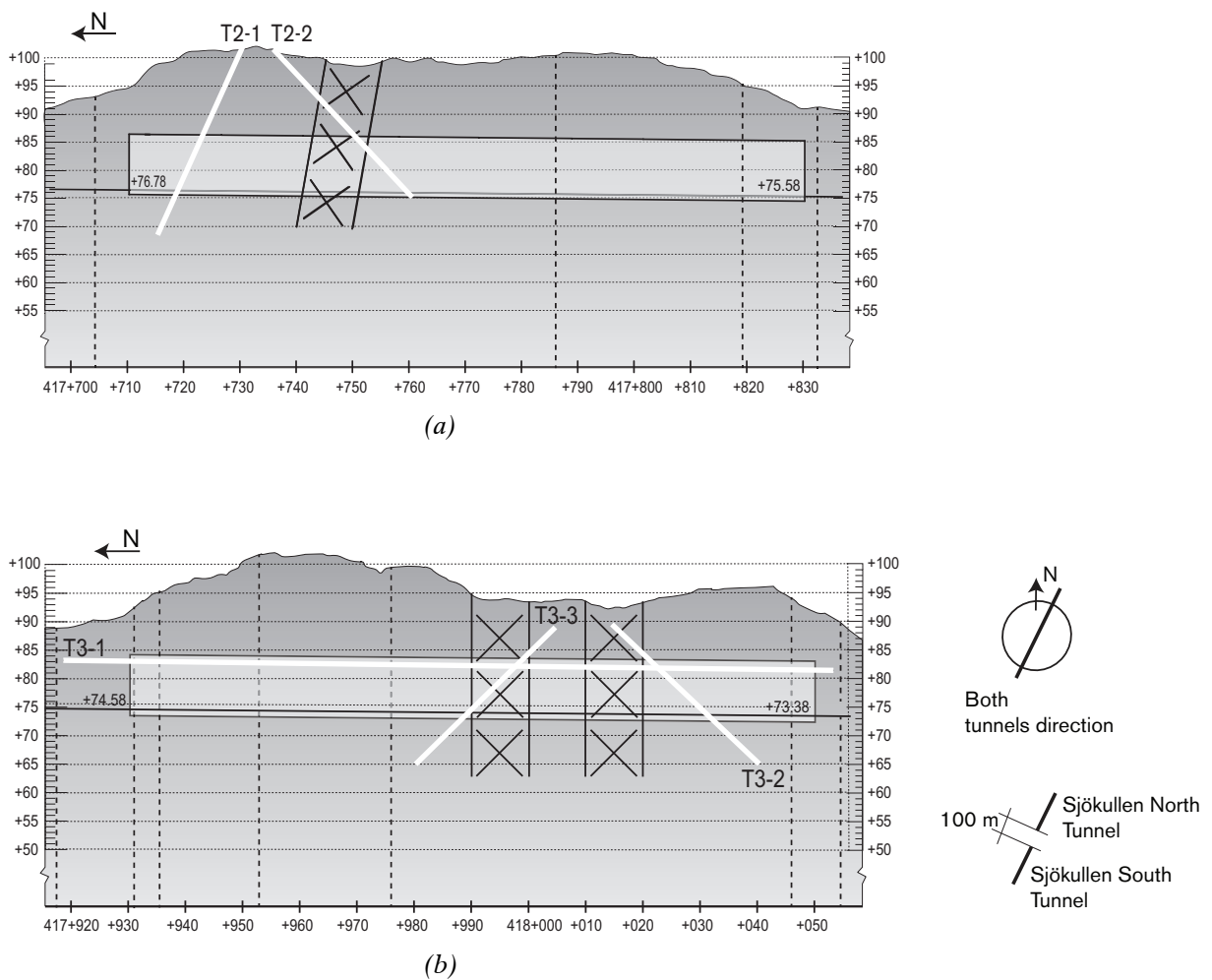

Figure 5.10   Profile illustration of the Sjökullen Tunnels, modified from the construction drawings: © Banverket (2010), Norway/Vänernbanan, Velanda-Prässebo section: (a) Sjökullen North Tunnel, (b) Sjökullen South Tunnel.

The choice of grouting material for the Sjökullen South Tunnel was a combination of cement and silica sol based on WPTs and the investigation consisted of design, follow-up and evaluation. Again, the design was based on the assumption that fractures behave as smooth, parallel plates although the concept corresponds to the illustration presented in Figure 3.4c in Section 3.3. The analysis that follows comes from two pre-investigation boreholes (T3-2 and T3-3) drilled along the Sjökullen South Tunnel, Figure 5.10b.

While the Sjökullen South Tunnel was grouted with a combination of cement and silica sol, the Sjökullen North Tunnel was grouted entirely with cement, although both designs aimed to prevent dripping. The rock type in the excavation area is mainly grey gneiss with elements of veined gneiss and amphibolites in different magnitudes. No inflow reduction was required or stated by the authorities thus the design aimed to minimise the dripping amount (Trafikverket, 2010a, 2010b).

Pre-investigations

Following the same procedure as in the Nygård Tunnel project, the fracture frequency per 3-metre section and the corresponding transmissivity were evaluated and are shown in Figure 5.11a and Figure 5.11b. The first 8 m in borehole T3-2 underwent no WPTs and was thus not included in the evaluation; as well as T3-3, which had only two sections included in the evaluation for the same reason. This data gave an average fracture intensity of $P_{10} = 3.8$ fractures/m and an approximated total transmissivity of $1.6 \cdot 10^{-5}$ m^2/s with a maximum transmissivity of $1.1 \cdot 10^{-5}$ m^2/s. Groundwater pressures were measured at 0.5 bar.
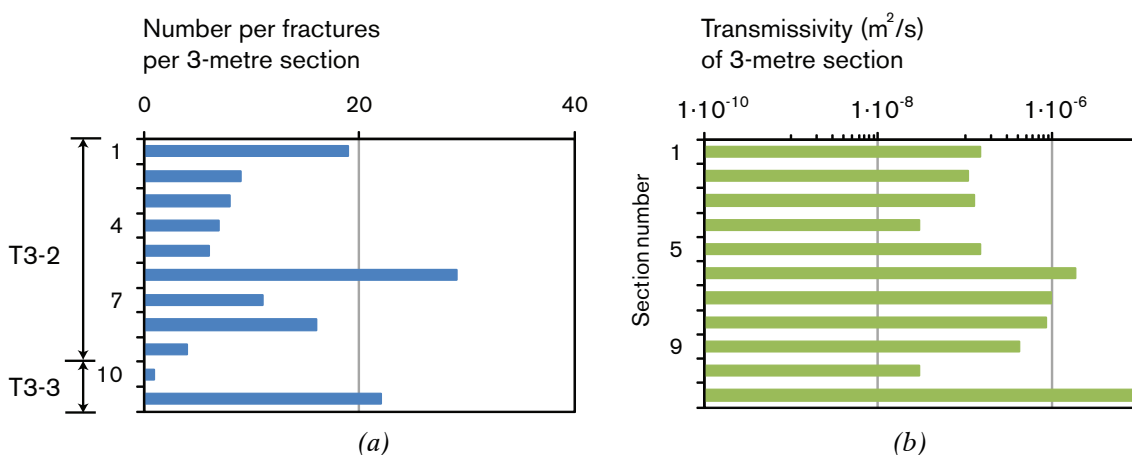

Figure 5.11   *Data gathered from two pre-investigation boreholes (T3-2 and T3-3). Each section is 3 m and the number of sections varies in each borehole: (a) Fracture frequency per 3 m-section, (b) Calculated transmissivities per 3 m-section.*

Fracture transmissivity and fracture aperture distribution

The evaluated Pareto distribution and calculated hydraulic aperture distribution is presented in Figure 5.12a and Figure 5.12b respectively. The coefficient (*-k*) obtained from the Pareto distribution after various iterations using the Newton-Rhapson iteration method is equal to 0.743, see Figure 5.12a.

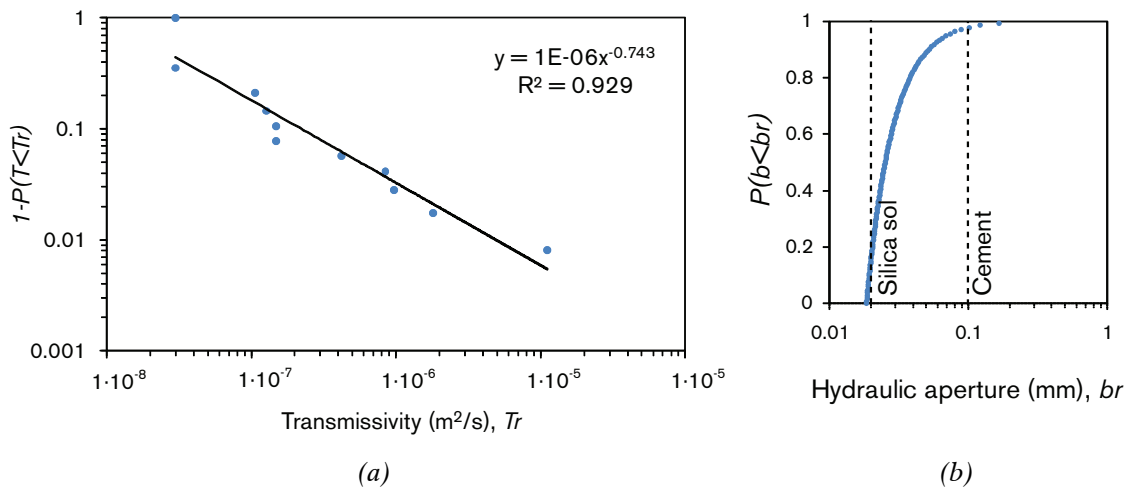*(a)*   *(b)*

Figure 5.12   *Evaluation of the pre-investigation boreholes T3-2 and T3-3: (a) Evaluated Pareto distribution from transmissivities of 3-metre sections, (b) Calculated hydraulic aperture distribution.*

Using this coefficient and the cubic law, the hydraulic aperture distribution is then calculated and goes from around 15 μm to 200 μm, see Figure 5.14. Within this range, 98% of the fractures have a hydraulic aperture less than 0.1 mm and around 16% of them have an aperture of less than 20 μm. This means that the use of only cement will have a limited sealing effect, and that silica sol would be a better option to seal fractures that are less than 0.1 mm in hydraulic aperture.

As in the Nygård Tunnel, the major contribution to the transmissivity of the borehole seems to come from a few wide fractures, and a comparison of the Pareto and hydraulic aperture distributions shows that the hydraulic apertures in the Sjökullen South Tunnel are wider than in the Nygård Tunnel, see Figure 5.3a in Section 5.1.

Layout, grout type and penetration distribution

The existing layout proposed by the consulting company was used with no further changes, see Figure 5.13, and the penetration length needed to have an overlap of at least 50% was calculated accordingly to it.
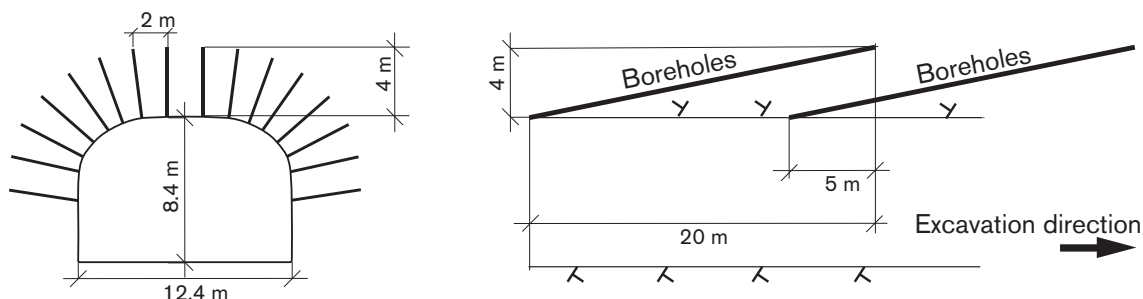

Figure 5.13   *Layout of the grouting boreholes for each fan in the tunnel, modified from the construction drawings: © Banverket (2010), Norway/Vänernbanan, Velanda-Prässebo section. Front view and lateral view of a cut made in the middle*

The penetration length, calculated injection of silica sol and cement for 20 minutes with a constant over-pressure of 1.2 MPa in each situation, is presented in Table 5.5. These results give an overlap of at least 50% between the end-points of the boreholes when a fracture with a 20 μm hydraulic aperture is taken into consideration.

Table 5.5   *Grout penetration calculated during injection into a fracture with 2D-flow for 20 min with an applied over-pressure (Δp) of 1.2 MPa*

	Hydraulic aperture [mm]	Penetration [m] in a fracture (2D-flow)
Cement	0.1	2.8
Silica sol	0.02	1.5

Grouting protocol

The design consisted of the injection of 16 boreholes located in the tunnel roof, as shown previously in Figure 5.13, where the use of silica sol was decided based on the results obtained from WPTs conducted in each borehole before grouting. The decision method consisted of using cement if the inflow obtained from WPTs was higher than 3 L/min (approximate inflow into a 0.1 mm fracture), and using silica when lower or zero inflows were obtained.

Table 5.6 shows a summary of the protocol used in each of the eight fans grouted in the Sjökullen South Tunnel. The tunnel is 120 m in length and three fans were grouted entirely with cement (Fans 1, 2 and 3) while the rest (five fans) used a combination of silica sol and cement. Recipe 2 (cement grouting) was used when a more viscous (dense) grout was needed; this was the case when large volumes of grout using recipe 1 were pumped into a single borehole during grouting.

Table 5.6   Summary of the grouting protocol used in each fan and in each borehole.

	Layout		
Number of boreholes per fan	16		
Distance between boreholes (end-points)	2 m		
Theoretical grouted zone around the tunnel	4 m		
Overlap between fans	5 m		
Borehole length	24 m		
Borehole diameter	64 mm		
Type of grout	Silica sol	Cement Recipe 1	Cement Recipe 2
Minimum fracture aperture to be sealed	20 μm	100 μm	100 μm
Gelling induction time	13 min	-	-
Gelling time	40 min	-	-
Yield strength	-	0.5 to 1 Pa	2 to 5 Pa
Density	-	1490 to 1510 kg/m^3	1570 to 1590 kg/m^3
Marshcone	-	33 to 37 s	40 to 44 s
Pumping over-pressure (Δp)	12 bar	12 bar	12 bar
Approximate ground water pressure	0.5 bar	0.5 bar	0.5 bar
Pumping time	20 min	20 min	20 min
Minimum calculated penetration length	1.5 m	2.8 m	2.8 m

In the Sjökullen North Tunnel, which is 120 m in length, eight fans were grouted entirely with cement using the same layout as the Sjökullen South Tunnel and the protocol comprised the cement part (recipe 1 and recipe 2), which is presented in Table 5.6. Since this tunnel was grouted entirely with cement, no data analysis was made prior to grouting, although it is used later when a hydrogeologic comparison is made.

Dripping

No hydraulic tests were conducted after grouting. The dripping characterisation and the placement of the geomembrane lining are thus used to show the grouting results. A characterisation of both tunnels made by the project leader (geologist on site) in May 2011 is presented in Figure 5.14 and Figure 5.15.

It is important to state that the first 20 m from the entrance in both tunnels were not characterised and consequently no dripping spots are shown in these sections.

It was expected that both entrances (portals) in both tunnels are quite fractured, since they are close to the ground surface, giving a large amount of dripping. It was decided that this leakage would be controlled by geomembrane lining from the beginning of the project.

In these characterisations the dripping spot locations are easily recognised and they were eventually covered by geomembrane lining (Karlsson, 2012). Figure 5.15 shows that the Sjökullen South Tunnel presents none or few dripping spots in the middle part, which is not the case in the Sjökullen North Tunnel. This is the most comparable section of the tunnel since both ends of the Sjökullen South Tunnel were grouted entirely with cement.
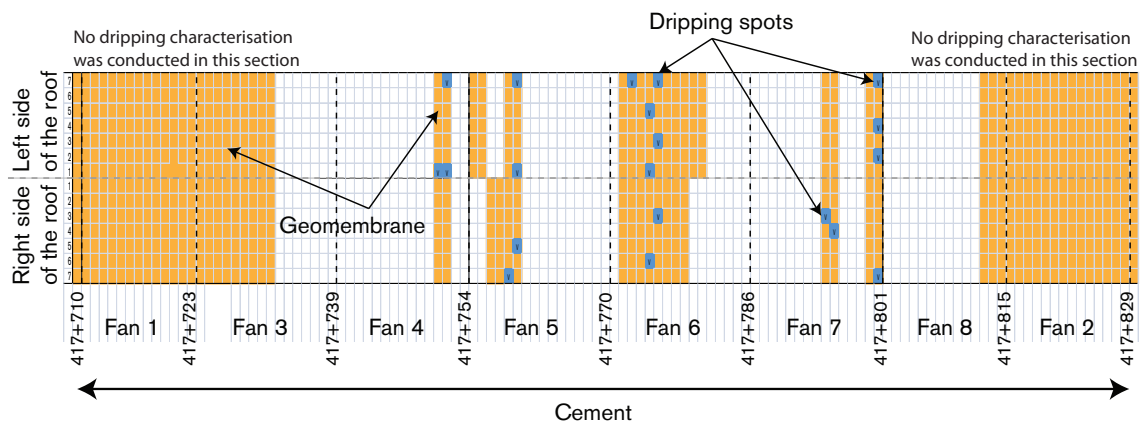

Figure 5.14   Drip characterisation in the Sjökullen North Tunnel conducted in May 2011. The dripping spot locations are marked by the blue areas. Fan extension is marked by the dotted lines and the geomembrane lining is marked by the orange areas.

Figure 5.15   Drip characterisation in the Sjökullen South Tunnel conducted in May 2011. The dripping spot locations are marked by the blue areas. Fan extension is marked by the dotted lines and the geomembrane lining is marked by the orange areas.
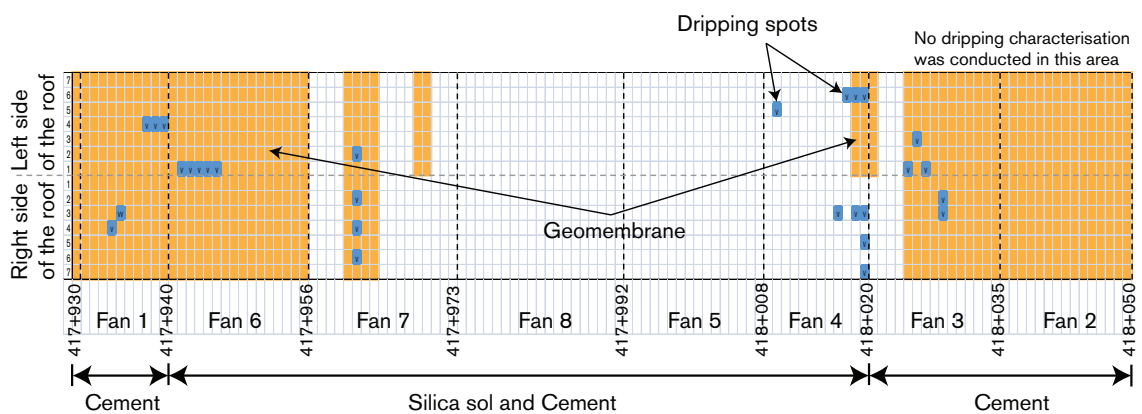
46

According to (Karlsson, 2012), approximately 70% of the roof in the Sjökullen North Tunnel is covered by geomembrane lining and around 50% of the roof in the Sjökullen South Tunnel is covered by geomembrane lining. This is shown in Figure 5.14 and Figure 5.15. Hence, a comparison of both dripping characterisations and the amount of geomembrane lining placed indicates that the use of silica sol and cement for grouting in the Sjökullen South Tunnel gave better sealing efficiency than was the case with cement only.

Dripping characterisation conducted in April 2011 in the Sjökullen South Tunnel shows 11 dripping spots, 52 humid areas distributed at both ends of the tunnel and quite a dry area in the middle of the tunnel, see Figure 5.16. This figure is similar to Figure 5.15, which is drip mapping conducted one month earlier, indicating similar results, and that the dry area located in the middle part was quite constant over a period of one month.
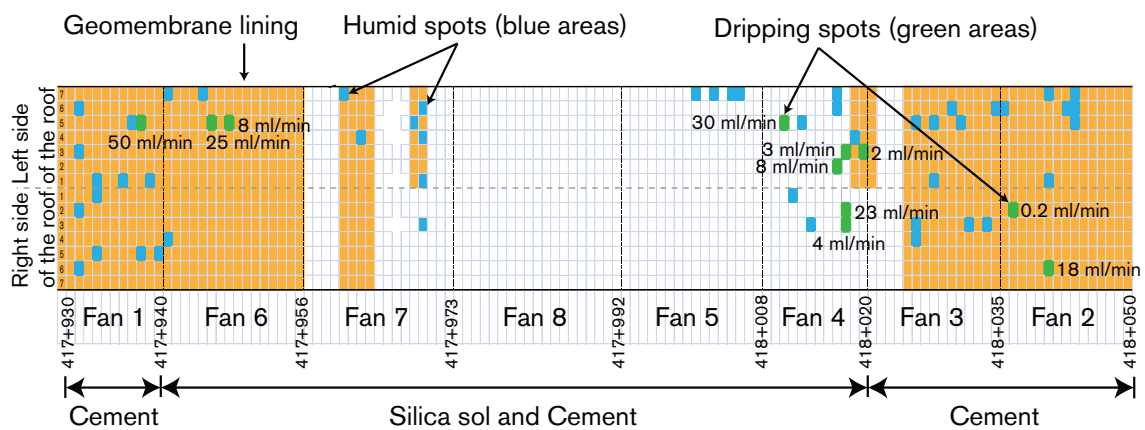

Figure 5.16   *Drip characterisation in the Sjökullen South Tunnel conducted in April 2011. The dripping and humid spot locations and flow are marked by the blue and green areas. Fan extension is marked by the dotted lines and the geomembrane lining is marked by the orange areas. Inflow measurements from quantifiable dripping spots in ml/min units are shown.*

It could be argued that both tunnels, located in sequence and 100 metres apart, do not present the same geology, although a comparison of the hydrogeologic characteristics shows that both tunnels are quite similar, see Figure 5.17. This figure compares the evaluated Pareto distributions of both tunnels from the pre-investigation borehole data.
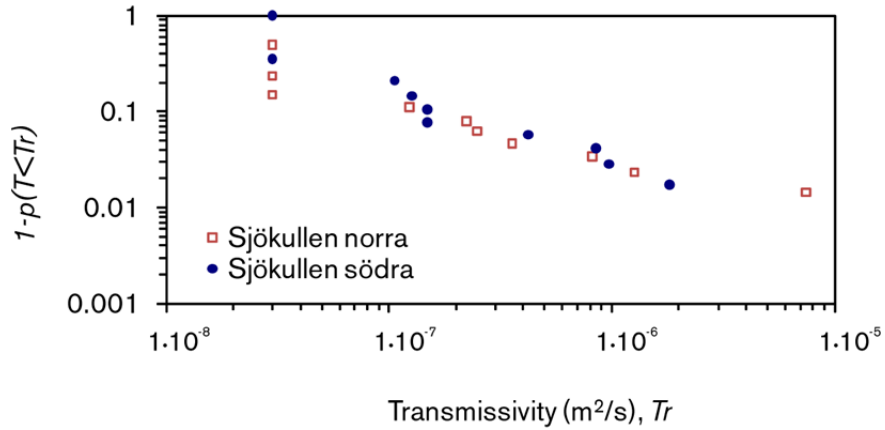
Figure 5.17   Comparison of the transmissivity Pareto distributions from the Sjökullen North Tunnel and the Sjökullen South Tunnel. The Pareto distribution is evaluated using transmissivities of 3-metre section (Pre-investigation).

The comparison of the dripping characterisation of both tunnels and the similarity in the fracture distribution indicates that the use of silica sol and cement for grouting produced better sealing efficiency that when cement only was used. As was done in the Nygård project, dripping characterisation at different times of the year, dry and wet seasons, is recommended to support the interpretations of the results obtained.

6   DISCUSSION

This chapter presents the conceptual model development and its verification. It presents an interpretation of the results obtained from the different study cases (Nygård, TASS and Sjökullen tunnels), gives opinions and explains the implication of the findings.

6.1   Conceptual model development

In the Nygård Tunnel study case, WPT data from all the grouting boreholes (five fans in 86 m of tested tunnel) is used to make a transmissivity variogram (Publication III). The experimental variogram is fitted using a model variogram (spherical), as in Figure 6.1a, and is used to interpret a correlation length, around 4 metres in this case. This correlation length is interpreted as an approximate size of the conductive areas.
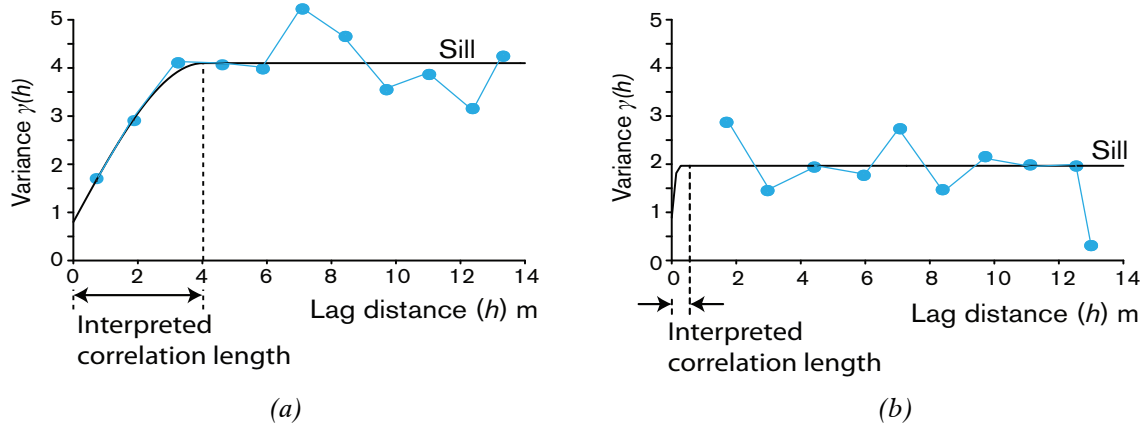

(a)   *(b)*

Figure 6.1   *Variogram of the base-10 logarithmic transmissivity values from WPTs from all fans in the studied section of the Nygård Tunnel (86 m); the dots are the experimental variogram and the curve is the fitted model variogram. The arrow shows an interpreted correlation length: (a) Before grouting and (b) After grouting.*

A separate variogram, shown in Figure 6.1b, is constructed for the same section of the tunnel, after the grouting was conducted, using WPT data from control boreholes located between the grouted boreholes in each fan. This variogram is very different from the first and shows that the rock mass has been altered substantially by the grouting. However, it is difficult to fit a suitable model; the data seems to show a very short or non-correlation length after grouting. It does

not exceed 1 m, which is shorter than the distance between neighbouring boreholes, indicating that there is no connectivity left between them. This means that most of the conductive areas were sealed during grouting.

Using the fitted variogram models (spherical) a kriging interpolation of the transmissivity values, taken from WPTs in each fan, is obtained. As an example, Figure 6.2a and Figure 6.2b are shown and correspond to the ungrouted rock in fans 1 and 5 respectively. Both figures show transmissive areas, e.g. areas A and C, and less transmissive areas, e.g. areas B and D, in different locations in each fan. These transmissive structures range from around 2 to 6 metres in size.
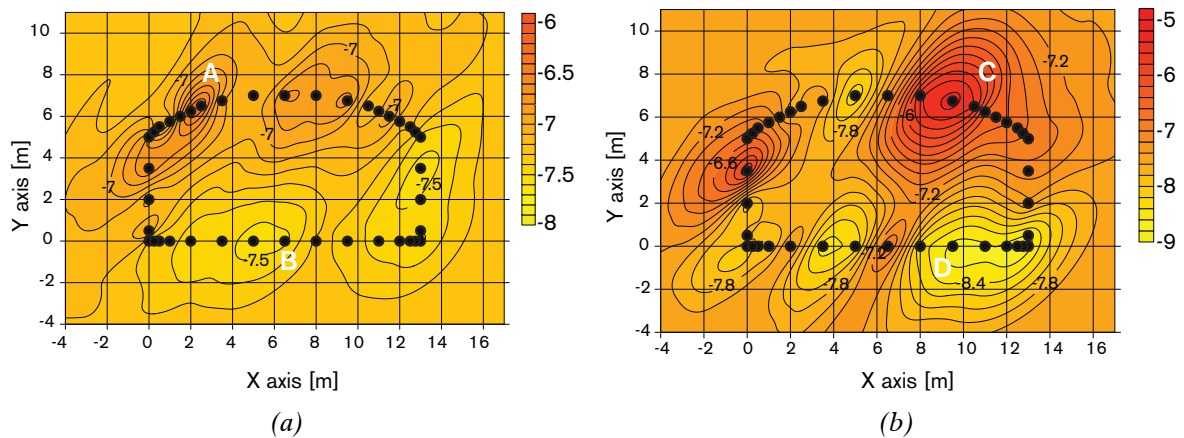

(a)   *(b)*

Figure 6.2   *Interpolation by kriging of the base-10 logarithmic transmissivity values obtained from WPTs before grouting. The filled dots represent the boreholes location and the scales represent the log transmissivity: (a) Fan 1 (b) Fan 5.*

A comparison of Figure 6.2a and Figure 6.2b gives the impression that fan 5, with transmissivity areas of 10^{-5} m^2/s, is more transmissive than fan 1, with areas of 10^{-6} m^2/s (highest transmissivity). On the other hand, both fans present areas with low transmissivity (10^{-8} m^2/s and 10^{-9} m^2/s). The kriging interpolations thus show that the analysed rock mass is composed of both transmissive and less transmissive areas with a characteristic size of approximately 2 to 6 metres.

After grouting, about 10 control boreholes were drilled in each fan and WPTs were conducted. These boreholes were located next to boreholes that showed high WPT results before grouting or which have a large grout-take. Using the fitted variogram models shown in Figure 6.1 an interpolation by kriging was made using the same technique as for the grouting fans. The transmissivity reduction in fans 1 and 5 due to grouting is thus obtained and is shown in Figure 6.3a and Figure 6.3b respectively (Publication III).
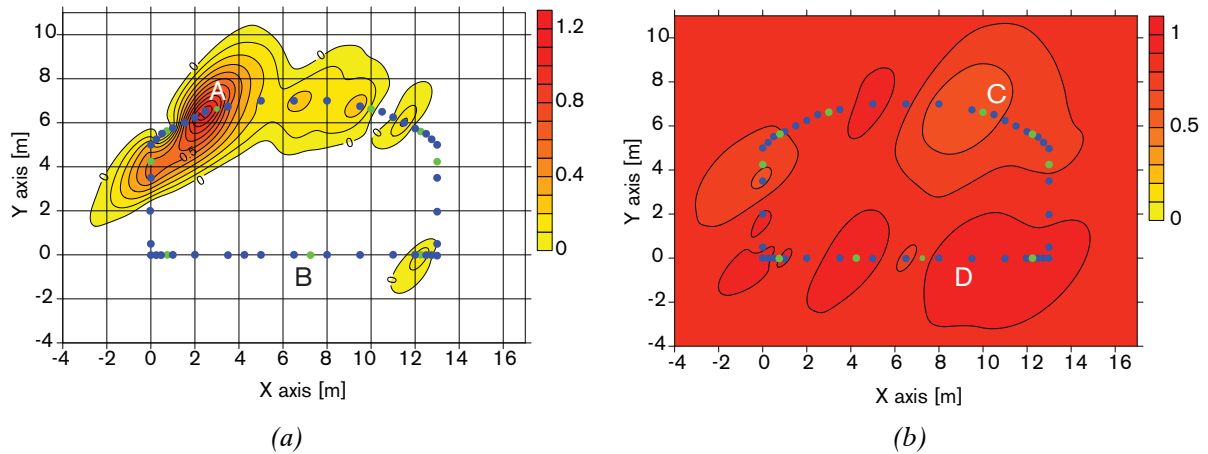
(a)   *(b)*

Figure 6.3   *Reduction of the base-10 logarithmic transmissivity values after grouting. Reduction measured as transmissivity field before grouting minus the transmissivity field after grouting. The white area represents no reduction in transmissivity. The black dots represent the borehole locations: (a) Fan 1 (b) Fan 5.*

It is clear from both figures that the sealing effect is different. Fan 5 has a greater sealing effect than fan 1, since it is shown that reduction took place in most of this fan, which is not the case in fan 1. In fan 1, it is the areas with high transmissivities that reveal a transmissivity reduction, such as area A in fan1 or areas C and D in fan 5. Thus, if the reduction in the transmissivity is compared with how the rock looked before grouting, it is evident that it is in the conductive parts of the fan where the grout has penetrated. This is natural since the grout penetration is proportional to the fracture aperture (see, e.g., Gustafson and Stille, 2005 and Funehag and Gustafson, 2008b).

Using the pressure volume time (PVT) data from each grouting procedure, the dimension of the flow injected into each borehole can be obtained, see Publication III. Figure 6.4 shows the dimensionality analysis of fans 1 and 5, where the results are marked as 1D if 1D-flow is obtained or 2D if 2D-flow is obtained. In Figure 6.4, crossed marks mean that the type of flow was not possible to determine. In all unmarked boreholes, there was no recorded grout-take beyond filling the grouting holes, either because they did not intersect transmissive fractures or because the fractures they intersected were already filled from other grouting holes. A disadvantage of this analysis is that it is not always easy to perform or to determine the dimension due to grout pump behaviour and measurement accuracy.
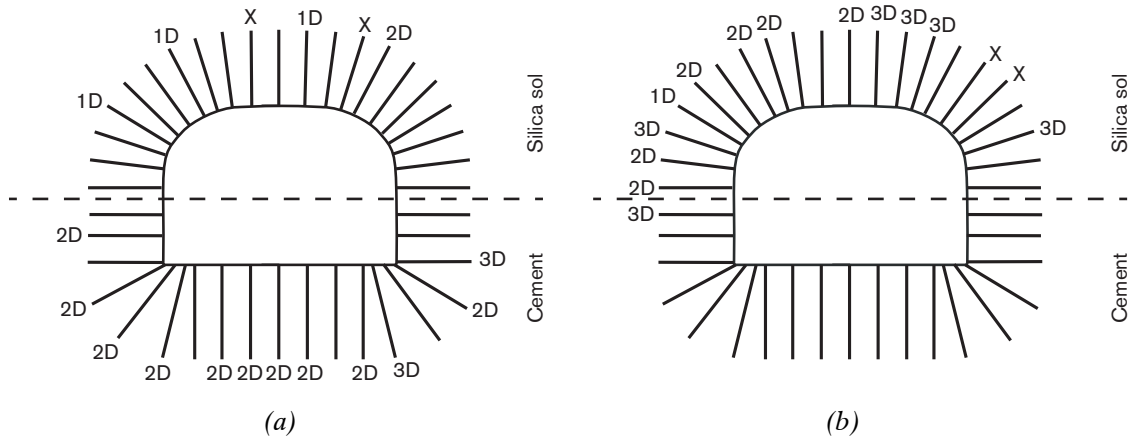
(a)   *(b)*

Figure 6.4   *Grout flow dimensionality results. Each hole was grouted with either silica sol or cement, and the grout flow dimension is marked, 1D or 2D. Cross marks represent boreholes that were not possible to examine. Unmarked lines represent boreholes with no grout-take: (a) Fan 1, (b) Fan 5.*

A quick view of Figure 6.4 shows that fractures with 1D- and 2D-flow are visible in both fans, but are unevenly distributed, and that a large number of the boreholes had no grout-take. Nevertheless, the examined boreholes suggest that the fracture network in both fans consists of a combination of fractures with 2D- and 1D-flow (channels).

By combining this dimensionality analysis with the variogram and kriging interpolation analyses, a conceptual model of the fracture structure or network is suggested, which is composed of fractures with transmissive patches (2D-flow fractures) connected by less pervious channels (1D-flow fractures), see Figure 6.5.
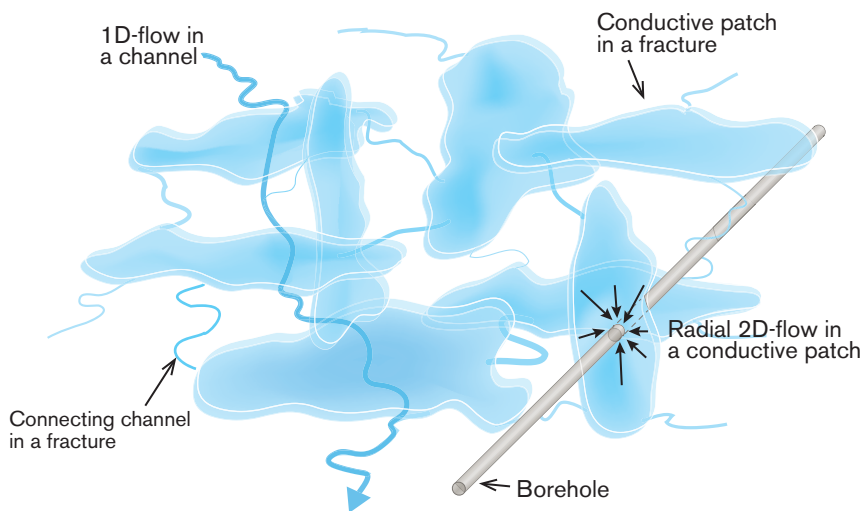

Figure 6.5   *Conceptual model of the conductive fracture system.*

This conceptual model provides a deeper understanding of the heterogeneity and connectivity of the fracture network and thus the groundwater conditions, not only in the roof but also around the tunnel contour. It also corroborates the assumption that a few conductive fractures (patches) make a major contribution to the transmissivity of the boreholes (Gustafson and Fransson, 2005).

In addition, closer examination of Figure 6.4a shows that fan 1 has a large number of boreholes intersecting channels with low perviousness and boreholes that took no grout during injection, resulting in a limited sealing effect, which is also shown by its transmissivity field, see Figure 6.3a. On the other hand, fan 5 seems to be composed mostly of fractures with 2D-flow and its transmissivity field shows a reduction in the whole fan. This means that the grouting takes place easily in the conductive patches where the transmissivity is good enough. This suggests that a rock mass with a more homogeneous fracture network is easier to seal than a rock mass with a more heterogeneous fracture network.

Furthermore, the conductivity of such a heterogeneous system is determined by the connecting channels rather than the conductive patches, since this is where most of the head drop will occur. Injection tests, such as WPTs, thus run the obvious risk of overestimating the bulk conductivity of the rock mass, since some of the boreholes are certain to penetrate conductive patches (radial 2D-flow) rather than channels (1D-flow) giving a high local transmissivity, see Figure 6.5.

6.2   Conceptual model verification and development

In order to verify the early developed conceptual model (data from the Nygård study case) in a similar crystalline rock type (diorite), data from the TASS project is used and a variogram, kriging interpolation and dimensionality analysis are conducted (Publication V). Data collected from fans 1 to 5 is used. These fans cover approximately 60 m of the tunnel.

A transmissivity variogram before grouting for all grouting boreholes, excluding fan 2, indicates a correlation length of around 2 m, see Figure 6.6a. As explained previously, this correlation length is interpreted as an approximate size of the connectivity in the rock mass. For comparison, a second variogram, shown in the same figure, has been constructed, including data from fan 2, indicating a correlation length of around 3 m. Fan 2 covers the 10 to 33.8 m section (length of the grouting boreholes) in the TASS Tunnel which is intersected by a transmissive fracture zone (structure 5). Both variograms show a fairly similar

interpreted correlation length (1 m of difference) of the ungrouted rock, which means that the fracture zone is masked by the hydraulic rock domain. Consequently, section 10 to 33.8 m is investigated further.
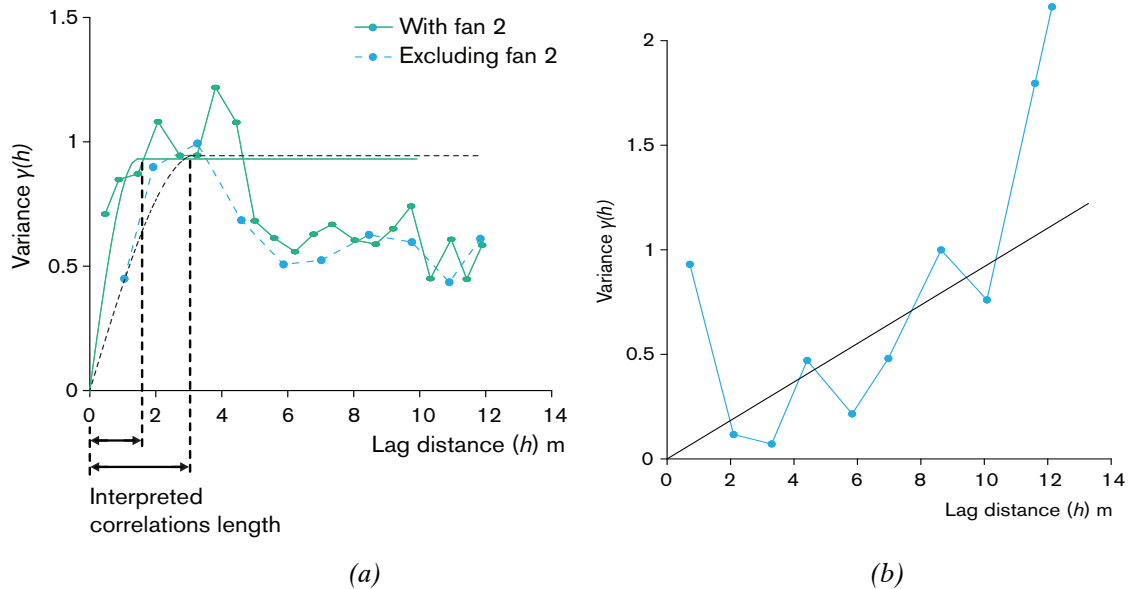

Figure 6.6   *Variogram of the base-10 logarithmic transmissivity values from WPTs from the first five fans in the TASS Tunnel. The dots represent the experimental variogram and the curve is the fitted variogram model (spherical). The arrow shows an interpreted correlation length (a) Before grouting and (b) After grouting.*

A third variogram, shown in Figure 6.6b, is constructed after the grouting of rounds A and B (the design covered three rounds of grouting, A, B, and C, where rounds B and C are used as control holes). This variogram is very different from the ones shown in Figure 6.6a, it shows no visible correlation length and even the fitting of a model is quite difficult. It is evident that it is not well connected, which means that most of the transmissive areas were sealed.

When comparing these results and results obtained from the Nygård study case, it could be asserted that in crystalline fractured rocks, such as diorite and gneiss, the connectivity behaviour of the hydraulic rock domain seems to be similar, although in this case the correlation length seems to be shorter. Using the fitted variogram models, a kriging interpolation of the transmissivity values in each fan is obtained and can be explored in Publication V. As an example Figure 6.7a and Figure 6.7b are shown. These figures correspond to the ungrouted rock transmissivity and the transmissivity reduction after grouting in fan 1 respectively.

Figure 6.7a shows areas that are transmissive, e.g. area A with a transmissivity of approximately 10^{-6} m^2/s, and areas than are quite tight, e.g. area B with a transmissivity of approximately 10^{-8} m^2/s, in different locations in this fan.
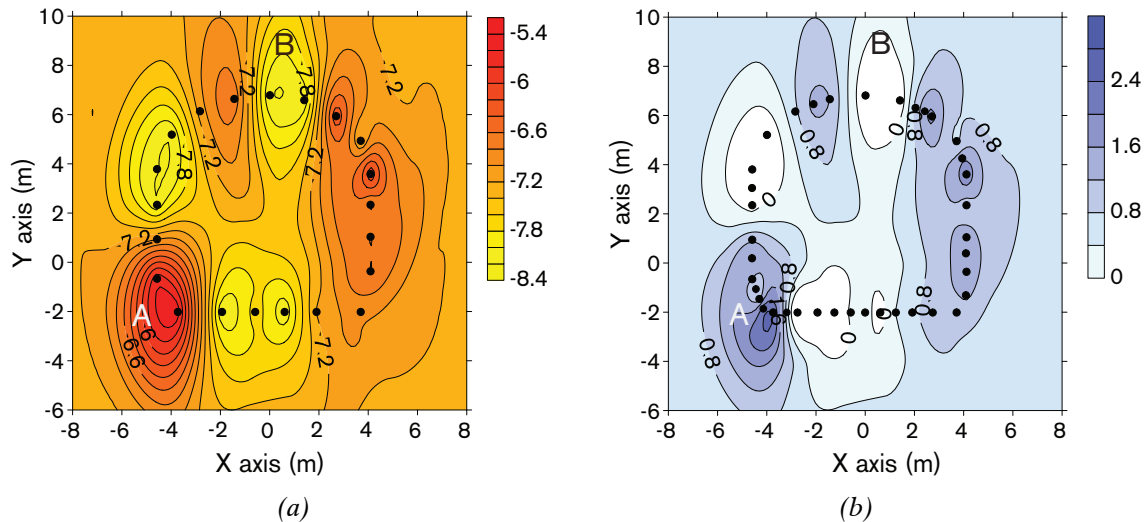

(a)   *(b)*

Figure 6.7   *Interpolation by kriging of the base-10 logarithmic transmissivity values obtained with WPTs in fan 1. The black dots represent the borehole locations: (a) Values before grouting, (b) Reduction of the transmissivity after grouting measured as transmissivity field before grouting minus the transmissivity field after grouting.*

Figure 6.7b, shows a transmissivity reduction of approximately three orders of magnitude in the highly conductive areas, such as the lower left-hand corner, area A. In the less transmissive areas, the reduction is small or none, such as in the middle part of the roof, area B. This means that the grouting took place in the conductive areas and the channelised areas were left unsealed due to the difficulty of intersecting them with the boreholes. This implies, as in the Nygård Tunnel, that the fracture structure in the hydraulic rock domain of the TASS Tunnel is composed by less transmissive channels connecting transmissive patches, which verifies the conceptual model developed in Section 6.1.

Additionally, a transmissivity variogram analysis of WPT data from section 10 to 33.8 m in the TASS tunnel has been obtained and is shown in Figure 6.8a (Publication VI). This section is crossed by a transmissive fracture zone (structure 5) with an estimated inflow between 25 and 42 L/min (Funehag and Emmelin, 2011). The fitted variogram model reveals a correlation length of approximately 8 metres, although interpretations of longer correlation lengths are also possible, indicating even greater connectivity in the analysed section.
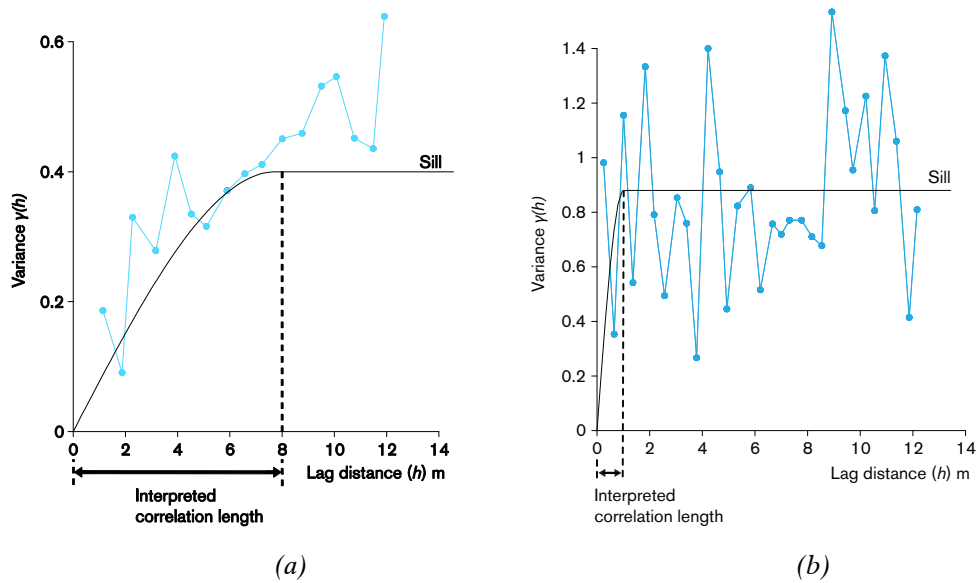
Figure 6.8   *Variogram of the base-10 logarithmic transmissivity values from WPTs from section 10 to 33.8 m in the TASS Tunnel. The dots represent the experimental variogram and the curve is the fitted model variogram (spherical). The arrow shows an interpreted correlation length (a) Before grouting and (b) After grouting.*

The transmissivity variogram obtained previously for fans 1 to 5 in the TASS tunnel indicated a correlation length of 3 m or 2 m depending if data from section 10 to 33.8 m was included or not, see Figure 6.6a. The longer correlation length of the studied section is presumably due to the continuity of the fracture zone that crosses this section. After grouting, the variogram in Figure 6.8b shows that the fit of a model is quite difficult, although if fitted the correlation length is quite short, less than 1 metre, implying that the fracture zone crossing the tunnel was sealed to a large extent.

The transmissivity field obtained from the kriging interpolation of section 10 to 33.8 m is based on the same transmissivity data used in the variogram analysis and uses the interpretations of correlation lengths of 8 m before grouting and 1 m after grouting. The transmissivity field of the ungrouted rock shows transmissive areas, such as the lower right-hand corner (area A). Other areas, such as the upper left-hand quarter (area B), are less transmissive, see Figure 6.9a. It is also possible to see the size of the transmissive structures, ranging from around 4 to over 8 meters in size.
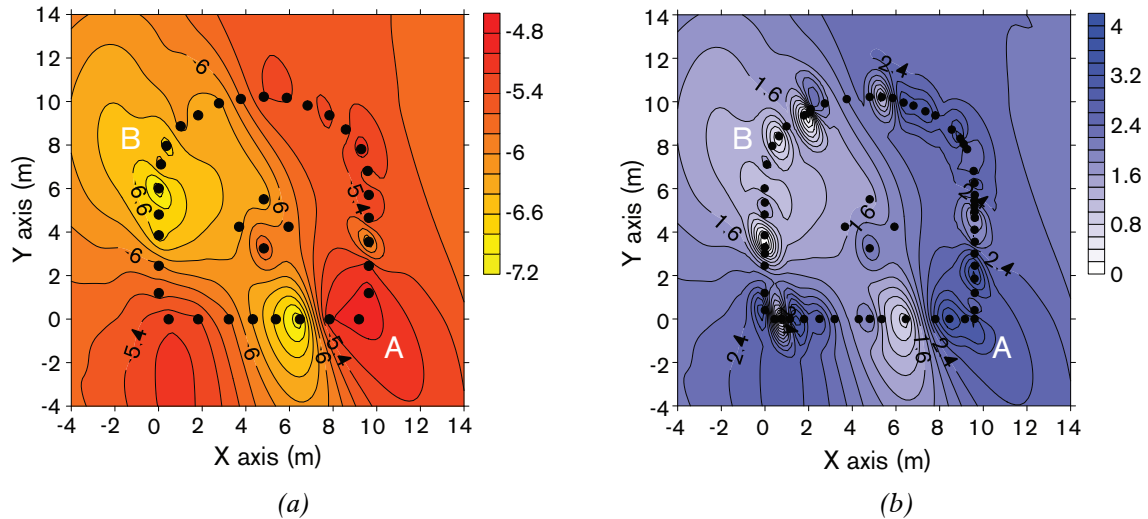
Figure 6.9   Interpolation by kriging of the base-10 logarithmic transmissivity values obtained with WPTs in fan 2 (fracture one). The black dots represent the borehole locations: (a) Before grouting; (b) After grouting of rounds 2A and 2B.

The diagram for kriging after grouting, Figure 6.9b, shows an overall reduction in transmissivity in the whole fan but with different magnitudes in different areas. The largest transmissivity reduction can be seen in the conductive areas, such as the lower right-hand corner area A, and is approximately three orders of magnitude. In the less transmissive areas, the reduction is less obvious, approximately one order of magnitude (area B). This shows an overall reduction in the fan transmissivity, which according to the results presented in Publication V is not the case in the rest of the fans.

As observed in the Nygård Tunnel, some holes did not take grout (beyond filling the grouting holes), either because they did not intersect transmissive fractures or because the fractures they intersected were already filled from other grouting holes. Of the holes that were examined, the result from the first round was that 2D cement and 2D silica sol grout spread was seen along the tunnel floor, with the same areas showing large transmissivity reductions in the transmissivity fields, while 1D silica sol grout spread was seen in the tunnel roof, e.g. in the upper left-hand quarter, area B, see Figure 6.10a.

The presence of many 2D flow features and the results from the kriging interpolation suggest that a fracture zone is quite homogeneous and presents mainly 2D-flow fractures. On the other hand, the hydraulic rock domain, which does not include the fracture zone, seems to be more heterogeneous and areas with no transmissivity reduction were obtained. This is analysed further in Section 6.3.
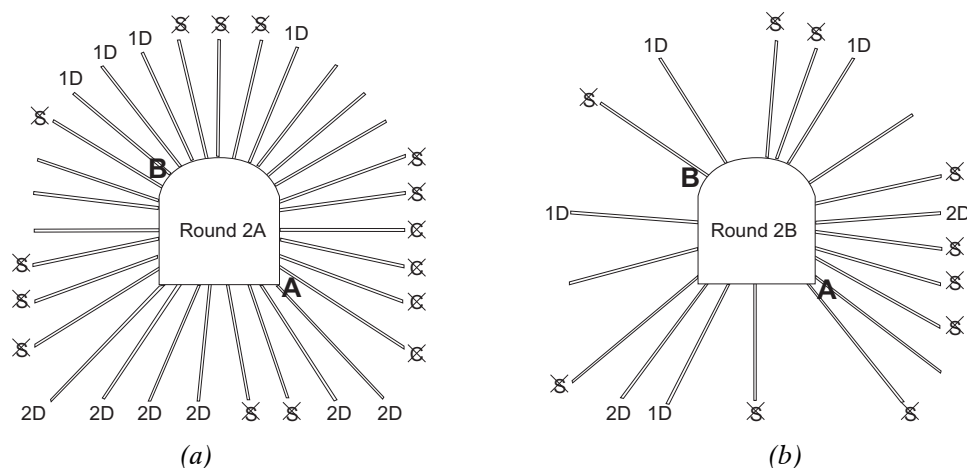
Figure 6.10   *Grout flow dimension in fan 2. Each hole was grouted with either silica sol or cement, and the grout flow dimension is marked 1D or 2D. A crossed S or C marks no grout-take of silica sol or cement. Unmarked boreholes were not possible to examine: (a) Values from round 2A (b) Values from round 2B.*

The evaluation of the second grouting round, see Figure 6.10b, shows few 1D-flows and only occasional 2D-flows. Hence, there does not seem to be any large remaining 2D-flow fractures although there are some channels left. Since the channels are less likely to be intersected by grouting boreholes, these may be more common than seen using the grouting boreholes. This comparison shows that almost all 2D features are sealed and only 1D features are left. One reason is that boreholes are most likely to intersect fractures perpendicular to the tunnel. Anisotropy may influence the tunnel inflow due to the existence of fractures running parallel to the tunnel.

6.3   Dripping and natural inflow test analysis

A comparison of the dripping distribution and the distribution of the natural inflow test values before grouting in the TASS tunnel is shown in Figure 6.11. The pre-investigation tests showed an inflow between 25 and 42 L/min before grouting Funehag and Emmelin (2011), which was reduced to 0.36 L/min after grouting (measured in the weir of this section). This quite large inflow reduction and a comparison of the NIT distributions and dripping distributions (largest reduction) clearly indicate that the grouting of the tunnel section crossed by the fracture zone had a better sealing effect than the rest of the hydraulic rock domain. This supports the results obtained using the previous variogram, kriging and dimensionality analysis, which shows that a more homogeneous rock is easier to seal (with the exception of extremely high water pressures, high hydraulic gradients or highly altered fault zones).
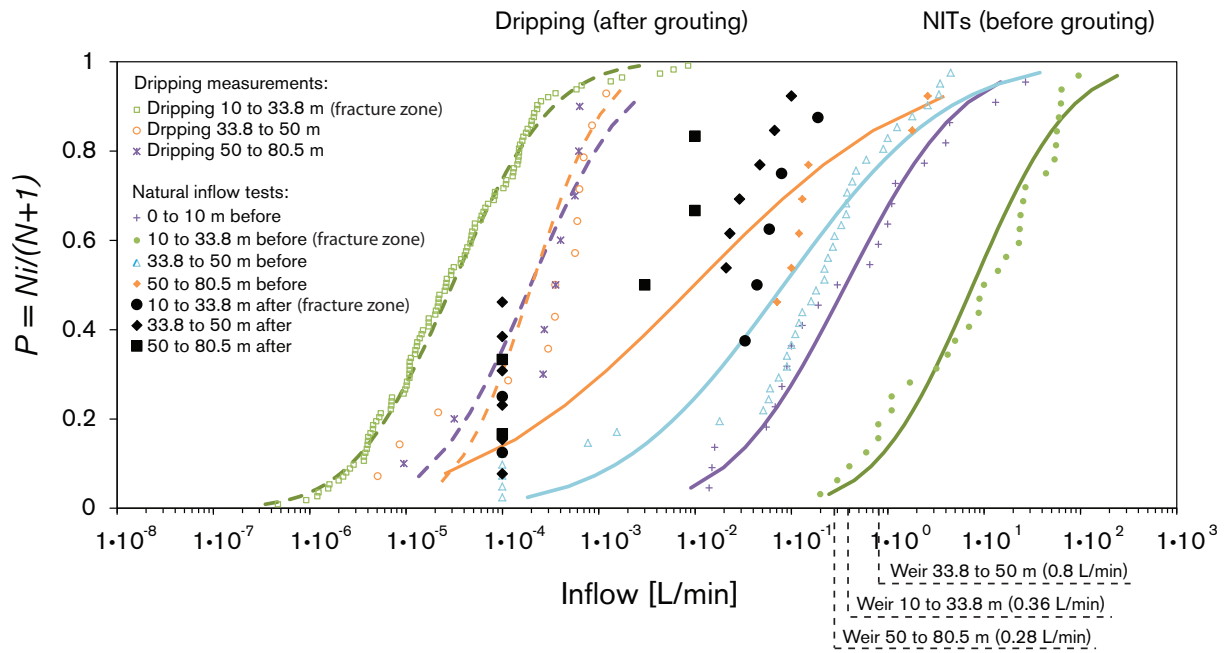
Figure 6.11   Measurements of the dripping areas characterised in all sections of the tunnel roof, and natural inflow tests (NITs) measurements conducted in the same sections before and after grouting. The fitted lognormal plots are also shown, excluding the NITs measurements after grouting. The inflows obtained at the monitoring weirs constructed at 10, 33.8 and 50 m are shown on the lower-right part of the figure.

If an analogy is made between a particle-size distribution curve in soils and the results presented in Figure 6.11, it can be said that the fracture zone before grouting behaves as a poorly graded soil (a narrow distribution, which means that most of the soil grains are the same size). This means that the fracture apertures do not differ too much in size (assuming that they are proportional to the inflow obtained) implying that the fracture zone is quite homogeneous and that it has more 2D features than 1D and is therefore easier to seal.

On the other hand, the various distribution curves of the inflow measurements in the rock domain before grouting are spread over a wide range (10^{-4} to 10 L/min), see Figure 6.11. If the same analogy is made, it can be said that the fracture zone after grouting behaves as a well graded soil (a wide distribution, which means that the soil grain sizes are distributed over a wide range). This means that the fracture apertures are distributed over a wide range and it is thus a more heterogeneous rock where 2D as well as 1D features are present. The existence of these channels makes grouting less effective since they are extremely difficult to intersect with the boreholes.

The dripping distributions in the roof after grouting shown in Figure 6.11 indicate that the remaining fractures that produce the dripping do not differ too much in inflow. They should thus in essence be 1D if the conceptual model is correct and the grout operation has sealed most of the transmissive patches (2D fractures).

Table 6.1   Total measured dripping inflows from different sections of the tunnel roof and measured inflows in the collecting weirs from every section, see Publication VII.

	10 to 33.8 m [mL/min)	33.8 to 50 m [mL/min)	50 to 80.5 m [mL/min)
Total from dripping	30	6	6
Total from weirs	360	800	280

Table 6.1 shows a comparison of the total inflow into the different sections from the dripping characterisation results and the inflow at the weirs. This comparison clearly shows that much of the inflow comes from the walls and floor of the tunnel. Fracture anisotropy and ventilation effects are possible reasons. Parallel fractures that were difficult to intersect with the grouting boreholes could have been left unsealed or opened as a result of a change in the stress conditions due to grouting. These fractures will transport water behind the tunnel wall to the lower parts of the tunnel and into the tunnel if intersected by horizontal fractures. Depending on the temperature and relative humidity of the air introduced by the ventilation duct, ventilation would reduce the inflow into the weirs due to evaporation. This would be more evident in the tunnel roof due to the location of the ventilation duct.

6.4   Unsaturated conditions, comments and observations

A conceptual model of the conductive fracture system is developed in Section 6.1, following analysis of the results from WPTs and PVTs, and is verified in Section 6.2. The conceptual model provides evidence of a hydraulically heterogeneous fracture system that is composed of fractures with transmissive patches connected by less pervious channels.

Before excavation, it is reasonable to assume that this conductive fracture system is in a saturated condition and that grouting will seal all the conductive patches intersected by the boreholes and some of the channels connected to those patches, although fractures with inconvenient orientations and channels not intersected by the boreholes will be left unsealed. This explains why, after well-executed grouting, dripping is still observed.

According to Cesano et al., (2000) minor leakages, such us dripping, are likely to be associated with the drainage of the water stored in the rock mass. The hypothesis is that with time these unsealed channels and patches become drained, creating successively more unsaturated conditions in the remaining unsealed fracture system, as shown in Figure 6.12.
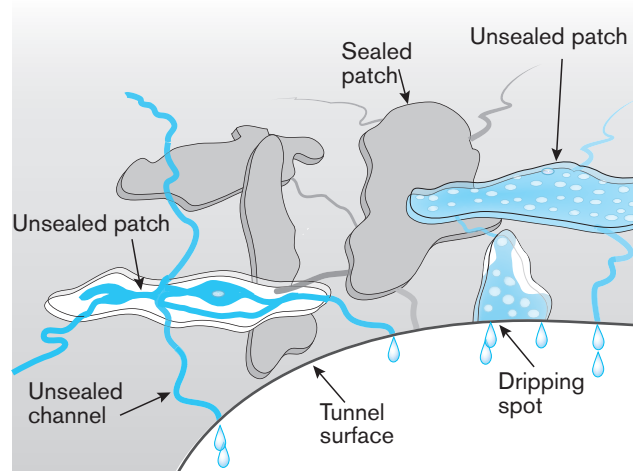

Figure 6.12   Conceptual model of the conductive fracture system after excavation of a tunnel in a crystalline rock.

In the Nygård Tunnel, the movement or fluctuation of the dripping spots after a time has been observed and measured on two occasions (September 27, 2008 and June 14, 2011). The observations show that the location of the dripping spots may not be constant over time. This dripping behaviour is commonly observed in most infrastructural tunnels. One reason for the dripping fluctuation could be the drainage and formation of preferential flow paths in wide fractures or open areas in a fracture, if the recharge is not sufficient to keep the system saturated, see Figure 6.12. This was observed on experiments conducted by Geller et al. (1996) and Geller et al., (1997) on plastic replicas. The experiments showed that the fracture the fracture orientation influenced the flow behaviour and that preferential flow paths have been formed.

Consequently, in unsaturated conditions the transmissivity of a fracture with a variable aperture is no longer constant. It decreases according to the degree of saturation, similar to porous media when it gets drained. This is supported by Jarsjö and Destouni (1998) model results, which indicate that the transmissivity of a system of interconnected fractures with different aperture characteristics decreases due to accumulation of gas in some of the fractures.

6.5 Design implications

Hydraulic aperture and grouting design

A conceptual model based on saturated 2D-flow in fractures was conceived at the beginning of this investigation. Consequently, all the equations used in the pre-investigation stage design and evaluation were based on the assumption that all fractures behave as smooth, parallel plates. A conceptual model was then developed with the aid of systematic observation, testing and a more in-depth analysis. This conceptual model describes a fracture system that is composed not only of fractures with 2D-flow (transmissive patches) but also of 1D-flow (less pervious channels).

The assumption that a fracture behaves like two smooth, parallel plates is quite appropriate for the design of the grouting procedure, but produces results that are a little on the conservative side (large safety margin) if channels are taken into account in the design. Figure 6.13a, which is based on the cubic law and Equation 2.1, shows the estimated fracture aperture, b, for a given flow, Q, and the difference in pressure, dh_w. Alternatively, Figure 6.13b which is based on the Hagen-Poiseuille law, Equation 2.2, shows the estimated channel diameter, d, for a given flow, Q, and the hydraulic gradient, dh/dl.
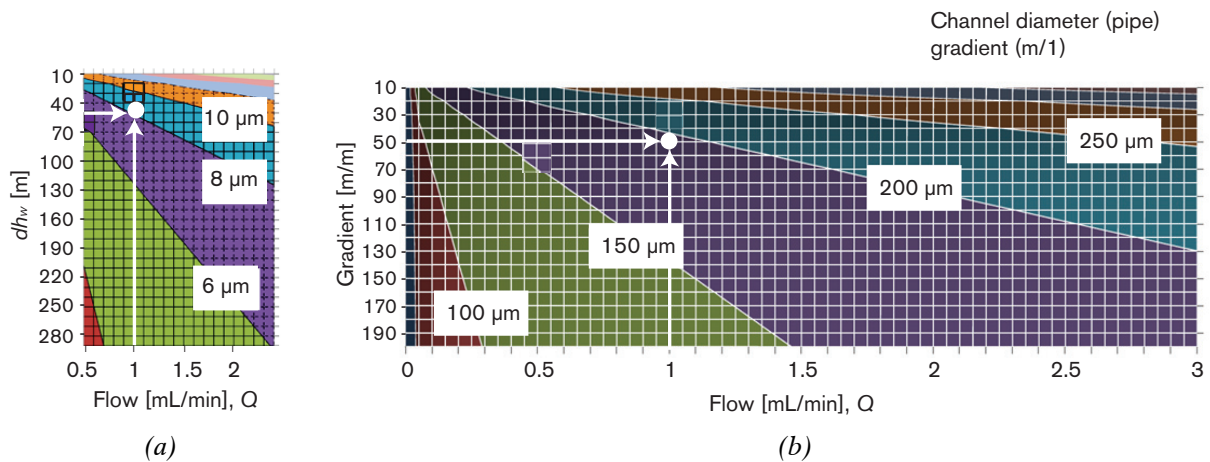
Figure 6.13   *Fracture aperture estimation (a) in a 2D-flow fracture, modified from (Fransson, 2009) and (b) in a channel (diameter).*

As an example, if a flow of 1 mL/min and a hydraulic head of 50 m are used in Figure 6.13a, the resulting fracture aperture would be approximately 8 μm. On the other hand, if Figure 6.13b is used, the resulting channel diameter would be just less than 200 μm, which is larger than the previously estimated fracture

aperture. In a grouting situation (if a channel is intersected) a larger penetration length of grout should be expected, given a larger overlap than the one used in the design. However, it must be taken into account that this is the most extreme case and that channels are exceptionally difficult to intersect with the grouting boreholes.

Connection between boreholes and selection of grout (penetrability)

Taking into account the measured volumes of grout injected, a cross-plot of the apparent injected volume of grout (the total pumped volume minus the borehole volume) and the hydraulic aperture calculated from WPTs is presented in Figure 6.14a (Nygård Tunnel) and Figure 6.14b (Sjökullen South Tunnel). Both graphs show negative volumes or very large volumes of injected grout in some of the boreholes. This behaviour is thought to be the result of a connection between boreholes, causing partial filling of boreholes adjacent to the borehole being grouted or some local heterogeneity intersected by the borehole. These features were observed in every grouting operation and are quite common in other projects.
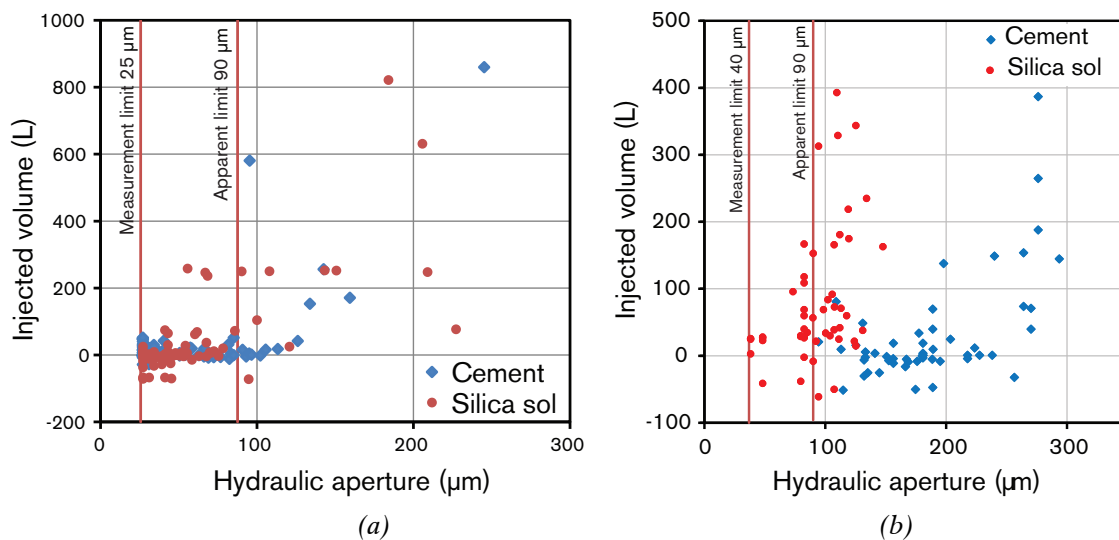
Figure 6.14   *Cross-plot of measured apparent injected volumes and hydraulic apertures calculated from WPTs. The measurement limit and apparent penetration limit for cement are also shown: (a) Values from Nygård Tunnel; (b) Values from Sjökullen South Tunnel.*

Apart from the connection of boreholes, Figure 6.14a shows that the injected volume when cement is used starts to rise above a maximum hydraulic aperture of around 90 μm ($b_{crit} \approx d_{95} \cdot 3 \approx 90$ μm when IC30 with a $d_{95} \approx 30$ μm is used).

Below this b_{crit} there is no substantial injected volume. According to a percolation hypothesis presented by Gustafson et al. (2009) these low volume intakes represent the filling of local channel clusters, leaving empty spaces in a fracture. This empty space could be filled by groundwater and generate dripping.

On the other hand, in both graphs a substantial volume of injected grout below the b_{crit} is visible when silica sol is used instead, complying with the design concept of sealing narrow fractures in order to reduce dripping. A field observation, shown in Figure 6.14a is that large volumes of silica sol, which is more expensive than cement, are used when wide fractures are intersected by the boreholes. The use of cement should thus be more efficient in this case, as was done in the Sjökullen South Tunnel study case, see Figure 6.14b.

Comparing Figure 6.14a and Figure 6.14b, it can be seen that when the grout is chosen according to the WPTs, as in Figure 6.14b, the use of large volumes of silica sol is reduced and narrow fractures that would only be partially filled with cement are filled by silica sol instead. Hence, grouting shows an improvement where the grout selection can be based on hydraulic tests. Furthermore, these hydraulic tests, in combination with control boreholes, can be used later to show the results of grouting and for analysis of the grouting procedure.

Strategies for waterproofing the tunnel roof

According to Lindblom (2010) and others, it is common during construction to carry out geological mapping, where geological features are illustrated and parameters such as the basis for the RMR and Q classifications are noted. If this geological map deviates too much from what was forecast at the planning stage, then modification can be made during construction.

As an example, Figure 6.15 combines the drip characterisation and geological mapping (drawn in situ by a geologist) conducted in the Nygård Tunnel. The information obtained from geological mapping visible in this figure is the foliation of the main rock type (gneiss), the existence of fractures that cross the entire roof, the location of some isolated features (greenstones) and the location of the dripping spots.

However, it is clear that this geological information alone is not sufficient to describe the fracture structure of the rock in the area studied for grouting purposes. In this thesis, the fracture system is described as a combination of connected transmissive patches and less pervious channels. Hence, there is a need for hydraulic tests in order to develop a conceptual model to understand the

fracture system and groundwater conditions around the tunnel. This is of particular interest if a drip sealing design is required. This information is then used as a basis for technical and practical strategies for waterproofing the tunnel roof.
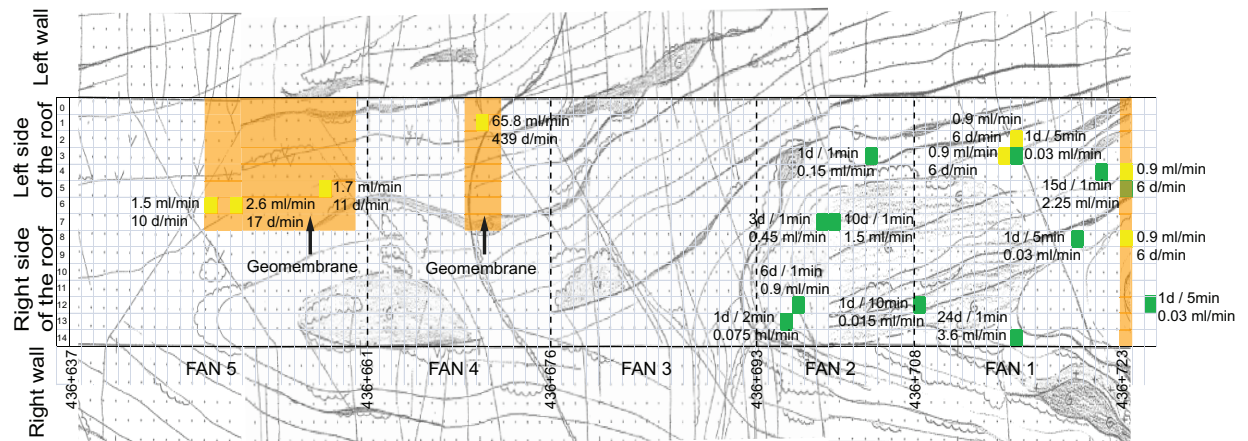

Figure 6.15   *Fracture and drip mapping of the studied section in the Nygård Tunnel. Inflow measurements from every dripping spot in d/min (drops per minute) and ml/min units are shown. The geomembrane lining location is also shown. Two drip characterisations are presented, the yellow squares represent the characterisation conducted on September 27, 2008, and the green squares represent the characterisation conducted on June 14, 2011.*

The analysis of the grouted section of the Nygård Tunnel showed that fan 5 was composed of more 2D-flow fractures than 1D-flow. It was more homogeneous and the transmissivity reduction was visible in the whole fan. The rock mass in fans 4 and 3 is the same, see Figure 6.15. The dripping characterisation seemed stable two years after, which means that the dripping spots did not move in the meantime. Hence, the extent and location of the geomembrane lining would appear to be confirmed.

In contrast, in areas that show few individual channels and are more heterogeneous, as in fan 1, the dripping does not seem to be stable. New dripping spots appeared after two years, which could be newly developed spots or old ones moving along fractures. In the same figure, the existence of a large greenstone element is visible (within fan 1 and 2). Hence, the use of geomembrane lining here is recommended highly, covering the whole of fans 1 and 2 and not only the areas where dripping was found following excavation. Further grouting would have a limited sealing effect due to difficulty intersecting the channels. This suggests that with the proper grouting technique and knowledge of the fracture

system and hydrogeology it would seem possible to propose technical and practical strategies for waterproofing the tunnel roof. This means a reduction in tunnel maintenance costs and fulfilment of the functionality requirements.

Low temperature effects on the remaining dripping

In the licentiate thesis, an analysis was made of how the remaining dripping influences the risk of ice growth and icicle formation in winter. This can be explored in detail in Butrón, (2009), although a summary of the main findings is presented below.

If the grouting is insufficient and fractures are left unsealed, it is expected that these remaining water-filled fractures will create ice growth on the periphery of the tunnel and at the interface between the lining and the tunnel. Ice growth will create problems since it causes progressive fracture growth when temperatures fall below freezing in winter. One reason is the migration of water into ice layers (lenses) in fractures, which grow larger with time (Talamucci, 2003 and Freitag and McFadden, 1997). This process is developed if the freezing process is not too rapid or if the overburden pressure is not remarkably high, as in shallow tunnels (Rempel, 2007). According to Walder and Hallet (1985), the migration of water, and thus the growth of ice layers, continues as long as the temperature remains between -4°C and -15°C.

Another reason for fracture growth is the freeze-thaw cycle when isolated rock fractures completely filled with water expand by 9% when freezing increases the transmissivity by approximately 30%. For this to happen, water in the periphery of the tunnel needs to have at least 70% saturation. This problem can be compared to some extent to frost heave in soils, which is most pronounced in silty soils where the combination of water supply by capillary suction and heat conduction at freezing produces maximum ground frost.

Icicles can also be created on the tunnel roof in freezing conditions. Their formation and growth depend on the heat loss into the air and the water supply rate (Szilder and Lozowski, 1993). High water supply rates do not create icicles, since the heat content of the water is high. Slight dripping does not create icicles either as they will freeze at the root, producing ice accumulation instead. Somewhere in between the icicles will grow considerably depending on the temperature and water supply rate (Makkonen, 1988).

7 CONCLUDING REMARKS

A summary of the main findings of the thesis and recommendations for further research are presented in this chapter.

7.1 Conclusions

A conceptual model of the groundwater hydraulic conditions around the tunnel contour in crystalline rocks has been developed. The general aim has been to describe the hydraulic processes before and after excavation for drip sealing grouting purposes. The methodology used to develop the conceptual hydraulic behaviour was created mainly using transmissivity determinations (Water Pressure Tests, WPTs) and analyses of the correlation structure from these data (semi-variogram analysis). The flowing dimensions in the fractures have also been found to be essential in order to describe the conductive system. With the aid of pressure, volume and time recordings (PVTs) conducted during grouting it has been possible to determine and indicate the dimensionality of the flow.

The conceptual model was verified using different analyses conducted in the Nygård Tunnel and Äspö TASS Tunnel. The studied fracture systems in the ancient brittle crystalline rock types are composed of transmissive patches (2D-flow fractures) connected by less pervious channels (1D-flow fractures). This conceptual model provides an understanding of the heterogeneity and connectivity of the fracture network and thus the groundwater conditions, not only in the roof but also around the tunnel contour. The model also corroborates the assumption that a few conductive fractures (patches) make a major contribution to the transmissivity of the boreholes, see e.g. (Gustafson and Fransson, 2005). Although boreholes are most likely to intersect fractures perpendicularly to the tunnel, anisotropy may influence the tunnel inflow due to the existence of fractures parallel to the tunnel.

The grouting design process used in the tunnelling projects followed a structured approach where pre-investigation boreholes provided parameters for the layout. The WPTs and PVT recordings mentioned above were used for the evaluation and analysis. The evaluation showed that the pre-excavation grouting design reduced the inflow and the environmental demands set in the different projects were fulfilled. However, dripping remained, making its characterisation very important when proposing a possible solution for its control.

The different analyses conducted and the reduction in the inflow, from 45 L/min to 0.36 L/min, show that a more homogeneous conductive structure, such as in a fracture zone, has mainly interconnected 2D-flow features. The grouting has a better sealing effect since boreholes have a greater chance of intersecting 2D features and are therefore comparatively easier to seal (with the exception of extremely high water pressures, high hydraulic gradients or highly altered fault zones). When this fracture zone was analysed, the correlation length of the ungrouted rock mass was at least 8 m and the transmissivity reduction obtained by grouting covered most of the analysed fan. On the other hand, a heterogeneous fractured rock mass, such as the rock domain between deformation zones, where both 2D- and 1D- flow features are present, was more difficult to seal. In this case the transmissivity reduction was more local since channels are extremely difficult to intersect with the boreholes and grouting is therefore less effective.

The correlation length of the ungrouted rock mass was a few metres before grouting and after grouting it was reduced, which can be interpreted as a reduction in the connectivity after grouting. It is proposed that what is left unsealed is a highly channelised system that would be extremely difficult to intersect with future boreholes. The flow, such as dripping, into a grouted tunnel section thus seems to be determined by these ungrouted channels.

Geomembrane lining and post-excavation grouting are possible solutions to the dripping problem, although particular attention needs to be given to the location. A tunnel section that presents quite a homogeneous fracture system and similar rock mass shows more stable dripping spot locations. Hence, targeted, post-excavation grouting or geomembrane lining is a possible solution under such conditions.

In contrast, when a tunnel section presents quite a heterogeneous fracture structure and different elements within the rock mass, the dripping spot locations seem to be unstable. Hence, the use here of geomembrane lining only is recommended since additional grouting would not have a visible effect as it would be extremely difficult to intersect the remaining channels. The extent of the lining needs to be judged carefully since dripping spots can move, as seen in the Nygård Tunnel study case.

After the excavation, an unsaturated condition in the remaining unsealed fracture structure is expected. This condition is expected to reduce the transmissivity and, depending on the fracture orientation, the formation of preferential flow paths

(see, e.g., Geller et al., 1996 and Geller et al., 1997). The observed movement of dripping spots in the tunnel roof after a period of time and the fluctuation of inflow are interpreted to be a consequence of unsaturated conditions in the fracture system after the excavation of the grouted tunnel section.

However, it can be concluded finally that with the proper grouting technique and knowledge of the fracture system and hydrogeology, it would seem possible to propose technical and practical strategies for waterproofing a tunnel roof, such as post-excavation grouting or geomembrane lining. These measures suggest a reduction in tunnel maintenance costs and fulfilling the functionality requirements.

7.2   Further research

This thesis, which deals with drip sealing grouting, has shown that the conductive system in the rock studied could be conceptualised by 2D- and 1D-flow fractures. A design based only on idealised 2D-flow fractures should thus be complemented with an analysis of 1D-flow fractures. It is suggested that the conductance related to channels, the distribution of the channelling and the cross-sections respectively, should be investigated further.

Unsaturated flow is a challenging and difficult topic. The two-phase flow behaviour in a fractured network remains to be investigated, as there is a need for modelling development.

The existence of a continuous axial or a more local excavation damaged zone, EDZ, at different locations along a tunnel could give rise to the possibility of hydraulic interaction with a tunnel. It is proposed that models for these conditions be elaborated on in more detail.

Parallel fractures that were difficult to intersect with the grouting boreholes could have been left unsealed or opened as a result of a change in the stress conditions. This will move water behind the tunnel wall to the lower parts of the tunnel and into the tunnel if intersected by horizontal fractures. There is a need for further investigation into linking up hydraulic tests, grout pumping and mechanical properties.

Christian Butrón

REFERENCES

AFTES, 1989. Recommendations for the treatment of water inflows and outflows in operated underground structures. Tunnelling and Underground Space Technology, Vol. 4, No. 3, pp. 343-407.

Andersson, J., Dverstorp, B., 1987. Conditional simulation of fluid flow in three-dimensional networks of discrete fractures. Water Resources Research, Vol. 23, No. 10, pp. 1876-1886.

Andrén, A., 2006. Degradation of rock and shotcrete due to ice pressure and frost shattering. Luleå University of Technology, Luleå, Sweden.

Andrén, A., 2008. Analys av tunnlar med vatten- och frost problem. Banverket, F07-15445/BA45, Sweden.

Asakura, T., Kojima, Y., 2003. Tunnel maintenance in Japan. Tunnelling and Underground Space Technology, Vol. 18, No. 2-3, pp. 161-169.

Axelsson, M., 2004. Mechanical tests on silica sol: An introductory study on material characteristics for silica sol. Department of Civil and Environmental Engineering, Chalmers University of Technology, Gothenburg, Sweden.

Axelsson, M., Nilsson, J., 2002. Sealing of narrow fractures in rock with use of silica sol: An introductory study on material characteristics and behaviour as a grout. Department of Civil and Environmental Engineering, Chalmers University of Technology, Gothenburg, Sweden.

Black, J. H., Barker, J. A., 2007. An investigation of "sparse channel networks": Characteristic behaviours and their causes, SKB R-07-35, Stockholm, Sweden.

Bockgård, N., Niemi, A., 2004. Role of rock heterogeneity on lateral diversion of water flow at the soil-rock interface. Vadose Zone Journal, Vol. 3, pp. 786-795.

Butrón, C., 2005. Mechanical Behaviour of silica Sol: Laboratory studies under controlled stress conditions during the first five months of hardening process. Department of Civil and Environmental Engineering, Chalmers University of Technology, Gothenburg, Sweden.

Butrón, C., 2009. Drip sealing of tunnels in crystalline rock: Pre-excavation grouting design and evaluation. Licentiate Thesis, Department of Civil and Environmental Engineering, Chalmers University of Technology, Gothenburg, Sweden.

Butrón, C., Axelsson, M., Gustafson, G., 2009. Silica sol for rock grouting: Laboratory testing of strength, fracture behaviour and hydraulic conductivity. Tunnelling and Underground Space Technology, Vol. 24, No. 6, pp. 603-607.

Butrón, C., Gustafson, G., Fransson, Å., Funehag, J., 2010. Drip sealing of tunnels in hard rock: A new concept for the design and evaluation of permeation grouting. Tunnelling and Underground Space Technology, Vol. 25, No. 2, pp. 114-121.

Cesano, D., Olofsson, B., Bagtzoglou, A. C., 2000. Parameters regulating groundwater inflows into hard rock tunnels: A statistical study of the Bolmen tunnel in Southern Sweden. Tunnelling and Underground Space Technology, Vol. 15, No. 2, pp. 153-165.

Chernyshev, S. N., Dearman, W. R., 1991. Rock fractures. Butterworth-Heinemann, London, UK.

Christiansson, R., Ericsson, L. O., Gustafson, G., 2009. Hydraulic characterisation and conceptual modelling of the Excavation Disturbed Zone (EDZ). ISRM International Symposium on Rock Mechanics, Rock Characterization, Modelling and Engineering Design Methods, Hong Kong.

Dingman, S. L., 2002. Physical Hydrology. Prentice Hall. New Jersey, USA.

Doe, T. W., Geier, J. E., 1990. Interpretation of fracture system geometry using well test data. OECD/NEA Internal Report of the Stripa Project, 91-03, SKB, Stockholm, Sweden.

Dverstorp, B., Andersson, J., 1989. Application of the discrete fracture network concept with field data: Possibilities of model calibration and validation. Water Resources Research, Vol. 25, No. 3, pp. 540-550.

Eklund, D., 2005. Penetrability due to filtration tendency of cement based grouts. Division of Soil and Rock Mechanics, Royal Institute of Technology, Stockholm, Sweden.

Eklund, D., Stille, H., 2008. Penetrability due to filtration tendency of cement based grouts. Tunnelling and Underground Space Technology, Vol. 23, No. 4, pp. 389-398.

Ericsson, L. O., Brinkhoff, P., Gustafson, G., Kvartsberg, S., 2009. Hydraulic features of the excavated disturbed zone: Laboratory investigations of samples taken from the Q- and S-tunnels at Äspö HRL. SKB R-09-45, Stockholm

Fetter, C. W., 2001. Applied hydrogeology. Prentice-hall, New Jersey, USA.

Follin, S., 1992. Numerical calculations on heterogeneity of groundwater flow. Department of Land and Water Resources, Royal Institute of Technology, Stockholm, Sweden.

Fransson, Å., 2001. Characterisation of fractured rock for grouting using hydrogeological methods. Department of Civil and Environmental Engineering, Chalmers University of Technology, Gothenburg, Sweden.

Fransson, Å. 2009. Selection of grouting material based on a fracture hydraulic aperture assesment. Get undeground: Nordic Symposium of Grouting, Helsinki, Finland.

Freitag, D. R., McFadden, T., 1997. Introduction to cold regions engineering. ASCE Press, New York, USA.

Funehag, J., 2007. Grouting of fractured rock with silica sol: Grouting design based on penetration length. Department of Civil and Environmental Engineering, Chalmers University of Technology, Gothenburg, Sweden.

Funehag, J., 2008. Injekteringen av TASS-tunneln: Delresultat tom september 2008. SKB R-08-123, Stockholm, Sweden.

Funehag, J., 2010. Personal communication. February 1, 2010.

Funehag, J., Emmelin, A., 2011. Injekteringen av TASS-tunneln: Design, genomförande och resultat från förinjekteringen. SKB R-10-39, Stockholm, Sweden.

Funehag, J., Gustafson, G., 2008a. Design of grouting with silica sol in hard rock - New design criteria tested in the field, part II. Tunnelling and Underground Space Technology, Vol. 23, No. 1, pp. 9-17.

Funehag, J., Gustafson, G., 2008b. Design of grouting with silica sol in hard rock: New methods for calculation of penetration length, part I. Tunnelling and Underground Space Technology, Vol. 23, No. 1, pp. 1 to 8.

Geller, J. T., Su, G., Holman, H.-Y., Conrad, M., Pruess, K., Hunter-Cevera, J. C., 1997. Processes controlling the migration and biodegradation of non-aqueous phase liquids (NAPLs) within fractured rocks in the vadose zone. LBLN-39996, UC-400, Earth Sciences Division.

Geller, J. T., Su, G., Pruess, K., 1996. Preliminary studies of water seepage through partially saturated rough-walled fractures. LBNL-38810, UC-403, Earth Sciences Division.

Gnirk, P., Gray, M., 1992. OECD/NEA International Stripa Project: Overview of the investigation 1981 – 1992. Presentations to SKB. Stockholm.

Gustafson, G., 2007. Dimensionality analysis for silica sol grouting. TN 2007-10-11, Unpublished.

Gustafson, G., 2009. Hydrogeologi för bergbyggare.

Gustafson, G., Fransson, A., Butrón, C., Hernqvist, L. 2009. Effective fracture aperture for grout penetration. Get underground: Nordic symposium of rock grouting, Helsinki, Finland.

Gustafson, G., Fransson, Å., 2005. The use of the Pareto distribution for fracture transmissivity assessment. Hydrogeology Journal, Vol. 14, No. 1-2, pp. 15-20.

Gustafson, G., Stille, H., 2005. Stop Criteria for Cement Grouting. Felsbau Rock and Soil Engineering, Vol. 23, No. 3, pp. 325-332.

Hakami, E., Larsson, E., 1996. Aperture measurements and flow experiments on a single natural fracture. International Journal of Rock Mechanics and Mining Sciences & Geomechanics Abstracts, Vol. 33, No. 4, pp. 395-404.

Houlsby, A. C., 1990. Construction and design of cement grouting: A guide to grouting in rock foundation. John Wiley & Sons, New Jersey, USA.

ITA, 1991. Report on the damaging effects of water on tunnels during their working life. Tunnelling and Underground Space Technology, Vol. 6, No. 1, pp. 11-76.

Jarsjö, J., Destouni, G., 1998. Groundwater degassing in fractured rock: Modelling and data comparison. SKB TR-98-17, Stockholm.

Jarsjö, J., Destouni, G., Gale, J., 2001. Groundwater degassing and two-phase flow in fractured rock: Summary of results and conclusions achieved during the period 1994-2000. SKB TR-01-13, Stockholm.

Karlsson, J., 2012. Sjökullentunnlarna dräner data. Personal communication January 17, 2012.

Kitanidis, P. K., 1997. Introduction to geostatistics: Application to hydrogeology. Cambridge University Press.

Kleinstreuer, C., 2003. Two-phase flow: Theory and applications. Taylor and Francis Books, New York, USA.

Kutzner, C., 1996. Grouting of rock and soils. A.A. Balkema. Rotterdam, The Netherlands.

Larsson, E., 1982. Groundwater flow through a natural fracture: Flow experiments and numerical modelling. Chalmers University of Technology, Gothenburg, Sweden.

Larsson, E., 1997. Groundwater flow through a natural fracture. Licentiate Thesis, Department of Civil and Environmental Engineering, Chalmers University of Technology, Gothenburg, Sweden.

Larsson, T., Zetterlund, M., 2004. Evaluation of water pressure tests in control boreholes as a method of appraising the grouting result: A case study of Nordlänken, Öxnered - Trollhättan. Master Thesis, Department of Civil and Environmental Engineering, Chalmers University of Technology, Gothenburg, Sweden.

Lindblom, U., 2010. Berbyggnad.

Lindstrom, M. 2009. Fracture mapping and geomembrane lining position in the Nygård tunnel. Personal communication, March 11, 2009.

Makkonen, L., 1988. A model of icicle growth. Journal of Glaciology, Vol. 34, No. 116, pp. 64-70.

Marsily, G. de, 1986. Quantitative hydrogeology: Groundwater hydrology for engineers. Academic Press, Orlando, USA.

Matheron, G., 1967. Eléments pour une théorie des millieux poreux. Masson et Cie, Paris, France.

Mitchell, J. K., 1981. Soil improvement - State-of-the-art report. Proceedings, 10th International Conference on Soil Mechanics and Foundation Engineering.

Myers, J., 1997. Geostatistical error management: Quantifying uncertainty for environmental sampling and mapping. John Wiley & Sons, New Jersey, USA

Persoff, P., Pruess, K., 1995. Two-phase flow visualization and relative permeability measurement in natural rough-walled rock fractures. Water Resources Research, Vol. 31, No. 5, pp. 1175-1186.

Rasmuson, A. S., 1978. Water flow in an unsaturated porous medium. Royal Institute of Technology, Stockholm, Sweden.

Rempel, A. W., 2007. Formation of ice lenses and frost heave. Journal of Geophysical Research and Earth Surface, Vol. 112, No. 2.

Rhén, I., Gustafson, G., Wikberg, P., 1997. Results from pre-investigations and detailed site characterization: Comparison of predictions and observations. SKB TR-97-05, Stockholm, Sweden.

Richards, J. A., 1998. Inspection, maintenance and repair of tunnels: International lessons and practice. Tunnelling and Underground Space Technology, Vol. 13, No. 4, pp. 369-375.

Richards, L. A., 1931. Capillarity conduction of liquids through porous mediums. Physics, Vol. 1, pp. 318-333.

Selroos, J.-O., Walker, D. D., Ström, A., Gylling, B., Follin, S., 2002. Comparison of alternative modelling approaches for groundwater flow in fractured rock. Journal of Hydrology, pp. 174-188.

Sigurdsson, O., 2009. Personal communication, March 18, 2009.

Snow, D. T., 1968. Rock fracture spacing, openings, and porosities. Journal of the Soil Mechanics and Foundation Division, Proceedings of The American Society of Civil Engineers, Vol. 94, pp. 73-91.

Szilder, K., Lozowski, E. P., 1993. Stochastic modelling of icicle formation. Proceedings of the International Conference on Offshore Mechanics and Arctic Engineering - OMAE, Glasgow, Scotland.

Talamucci, F., 2003. Freezing processes in porous media: formation of ice lenses, swelling of the soil. Mathematical and Computer Modelling, Vol. 37, No. 5-6, pp. 595-602.

Trafikverket, 2010a. Norge/Vänernbanan, Velanda-Prässebo section: PM hydrogeologi.

Trafikverket, 2010b. Norge/Vänernbanan, Velanda-Prässebo section: Ingenjörsgeologisk prognos.

Trafikverket, 2011a. Deletapper om BanaVäg i Väst. Retrieved October 31, 2011 from http://www.trafikverket.se/Privat/Projekt/Vastra-Gotaland/BanaVag-i-Vast/Deletapper/.

Trafikverket, 2011b. Project BanaVäg i Väst. Retrieved October 31, 2011 from http://www.trafikverket.se/Privat/Projekt/Vastra-Gotaland/BanaVag-i-Vast/Deletapper/Velanda-Prassebo/.

Tsang, C. F., Neretnieks, I., 1998. Flow channelling in heterogeneous fractured rocks. Reviews of Geophysics, Vol. 36, No. 2, pp. 275-298.

Tsang, C. F., Tsang, Y. W., Hale, F. V., 1991. Tracer transport in fractures: Analysis of field data based on a variable-aperture channel model. Water Resources Research, Vol. 27, No. 12, pp. 3095-3106.

Tsang, Y. W., Tsang, C. F., 1989. Flow channelling in a single fracture as a two-Dimensional strongly heterogeneous permeable medium. Water Resources Research, Vol. 25, No. 9, pp. 2076-2080.

Walder, J., Hallet, B., 1985. A theoretical model of the fracture of rock during freezing. Geological Society of America Bulletin, Vol. 96, No. 3, pp. 336-346.

Wang, J. S. Y., Bodvarsson, G. S., 2002. Unsaturated zone testing at Yucca Mountain: Then and now. The Geological Society of America, Denver, USA.

Warner, J., 2004. Practical handbook of grouting. John Wiley & Sons, New Jersey, USA.

Verruijt, A., 1970. Theory of groundwater flow. Gordon and Breach Science Publishers.

Winberg, A., Andersson, P., Hermanson, J., Byegård, J., Cvetkovic, V., Birgersson, L., 2000. Final report of the first stage of the tracer retention understanding experiments. Äspö Hard Rock Laboratory, Stockholm, Sweden.

Christian Butrón